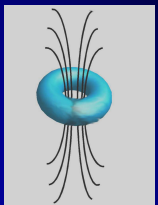


Biomagnetism:

Detection and Imaging Weak Magnetic Fields from the Human Body



Senior Scientific



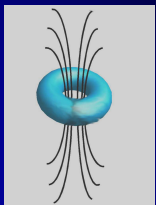
The University of New Mexico

Senior Scientific, LLC:

A private business with NIH SBIR funding.

Primary Mission: Disease detection using magnetic nanotechnology.

PI: Edward R. Flynn, PhD Physicist



Senior Scientific

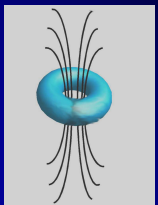


The University of New Mexico

Outline of Talk

Detection and Imaging of Weak Biomagnetic Fields

- 1) SQUID Sensors
- 2) Experimental Apparatus
- 3) Imaging the Brain
- 4) Imaging the Mind
- 5) Detection and Imaging Disease



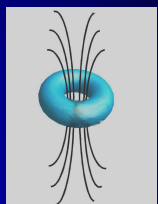
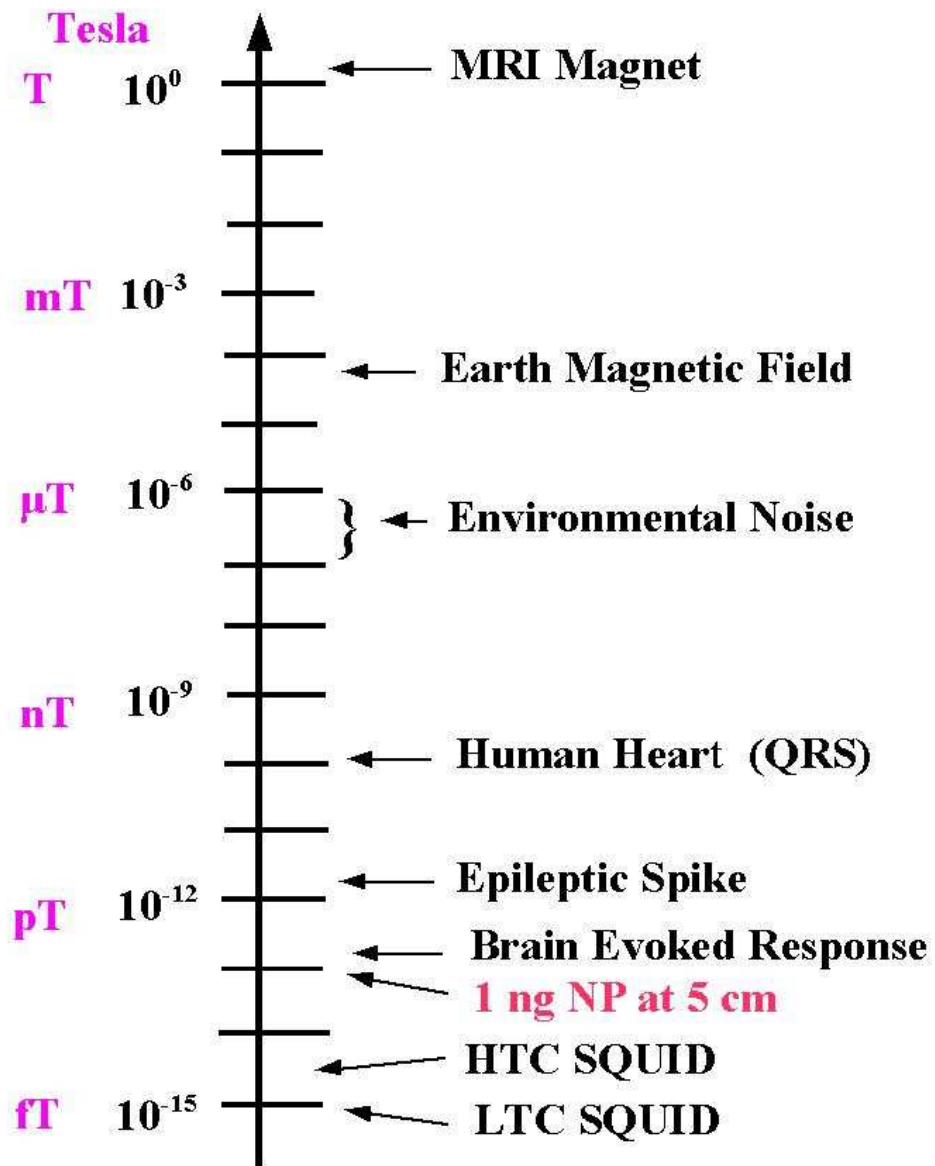
Senior Scientific



The University of New Mexico

Magnetic Field Strengths of various sources and Sensor Sensitivities

Magnetic Field Strength



Senior Scientific



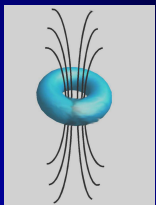
The University of New Mexico

MEG

Magnetoencephalography

Measurement of the natural magnetic fields
From the brain arising from neuronal currents

A: Instrumentation



Senior Scientific



The University of New Mexico

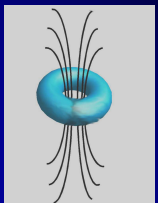
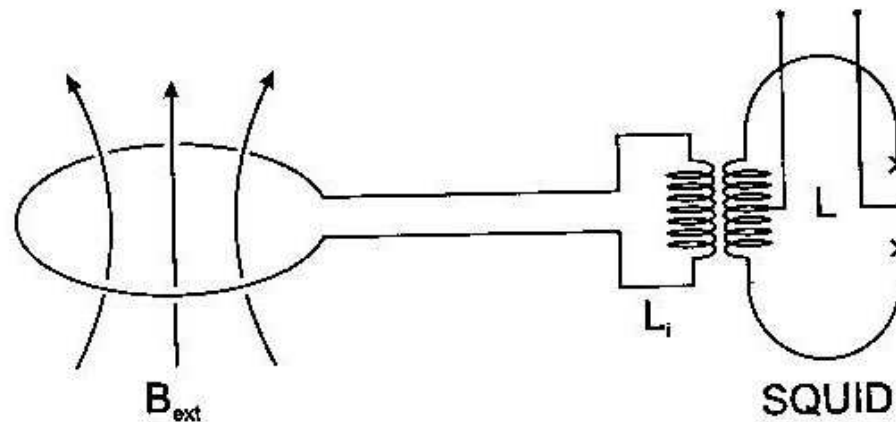
What is a SQUID?

Superconducting Quantum Interference Device (SQUID)

Quantum Mechanical (Josephson) Tunneling in a Superconductor

Sensor must have no resistive noise so superconducting material is used.

LTC SQUIDS are sensitive down to ~ 3 fT

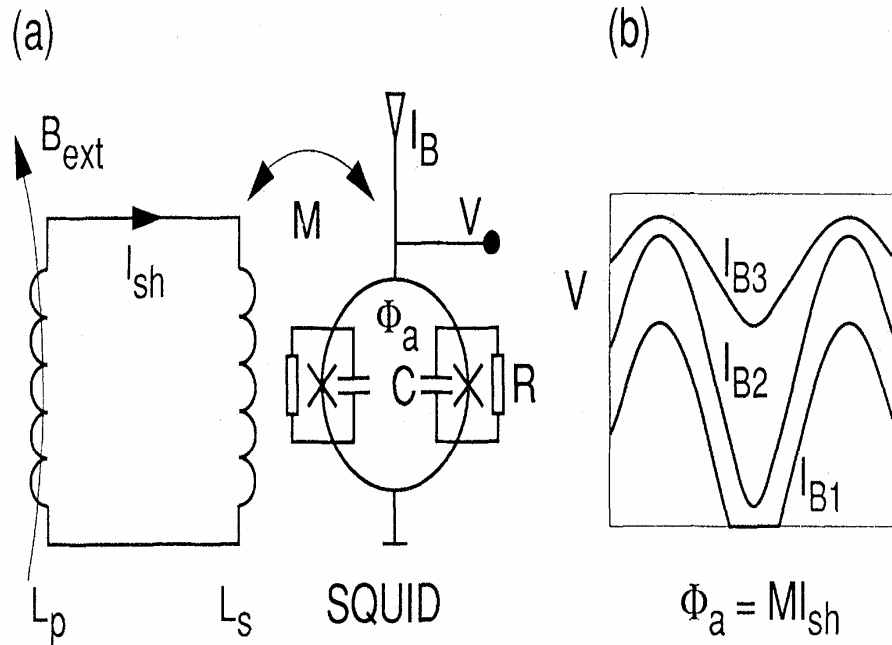


Basics of SQUID Operation

$$I = I_c \sin\theta ,$$

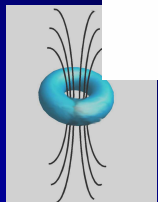
$$\frac{\partial\theta}{\partial t} = 2\pi V \frac{2e}{h} = \frac{2\pi V}{\Phi_0}$$

Josephson Equations: Θ is phase across junction, I =current, V = junction voltage, $\Phi_a = h/2e=2.07$ fWb (flux quanta)

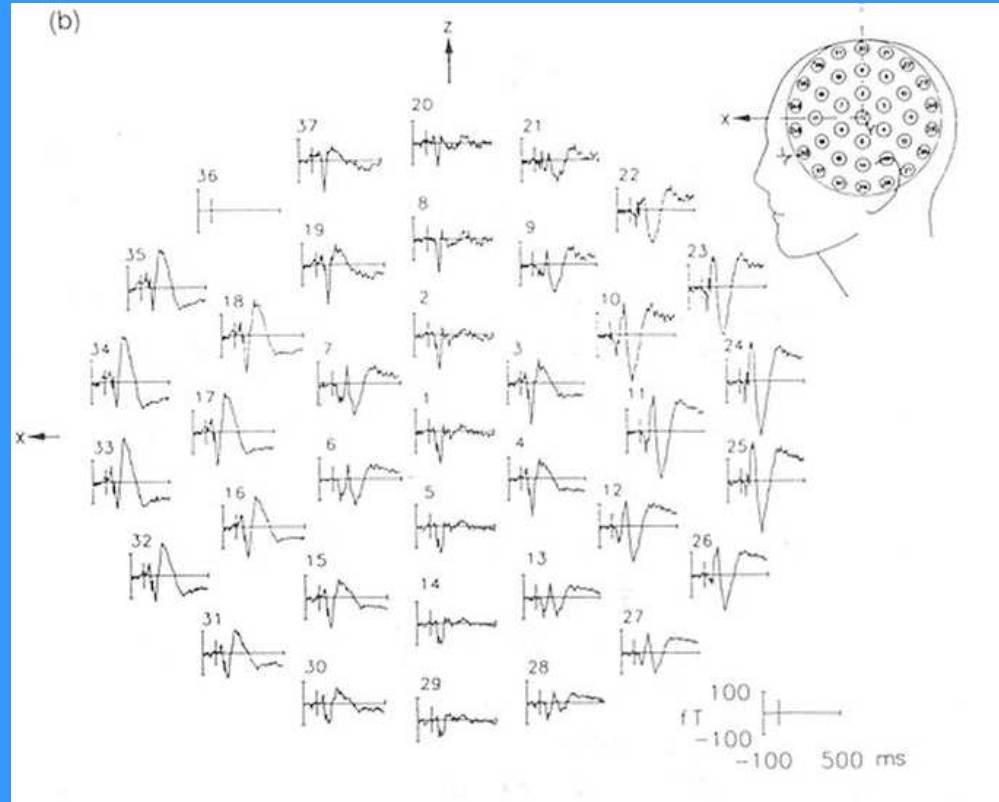
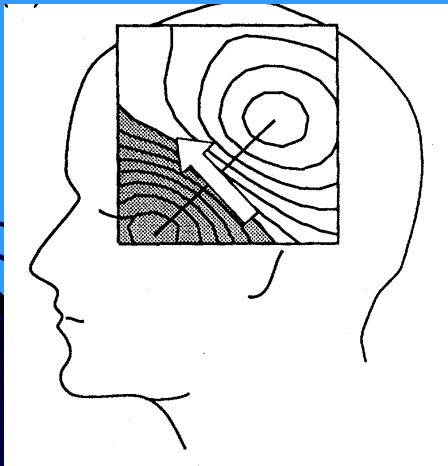
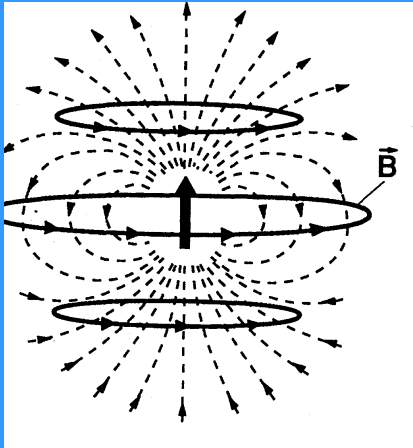


(a) Schematic diagram of DC SQUID, L_s is superconducting flux transformer

(b) Voltage across SQUID depends on bias I , and is periodic function of the incident flux Φ_a .

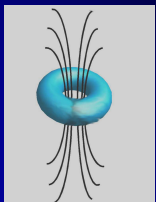


Principles of MEG



Field amplitude vs time for a sensor array - Evoked Response

Current Dipole



Senior Scientific

Matti Hämäläinen, Britta Hari, Risto J. Ilmoniemi, Jukka Knutila, and Olli V. Lounasmaa

to noninvasive studies of the working human brain
 Magnencephalography—Theory, instrumentation, and applications

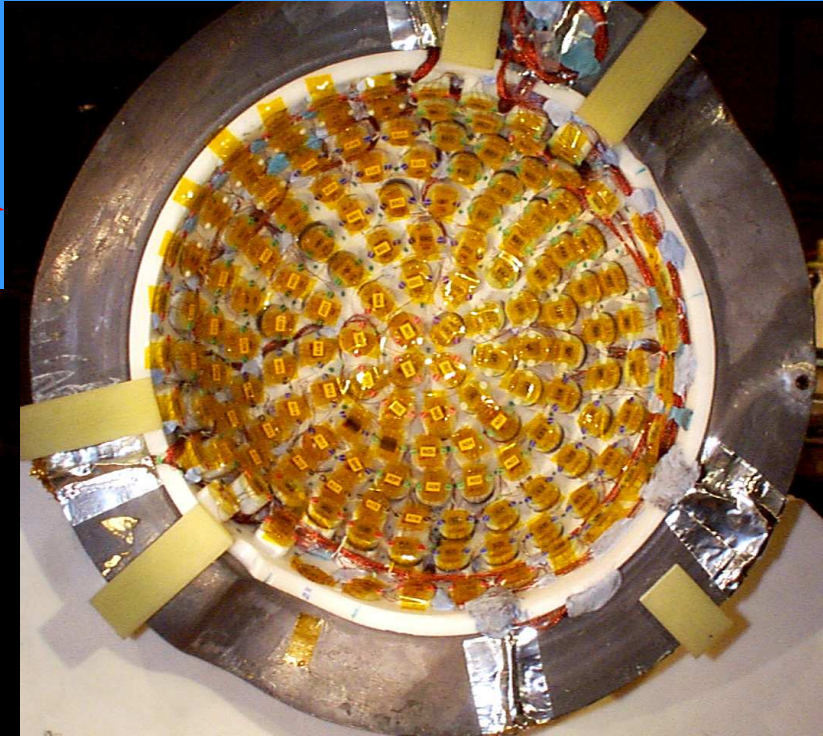
Reviews of Modern Physics, Vol. 65, No. 2, April 1993



The University of New Mexico

The SISG MEG System

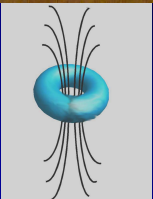
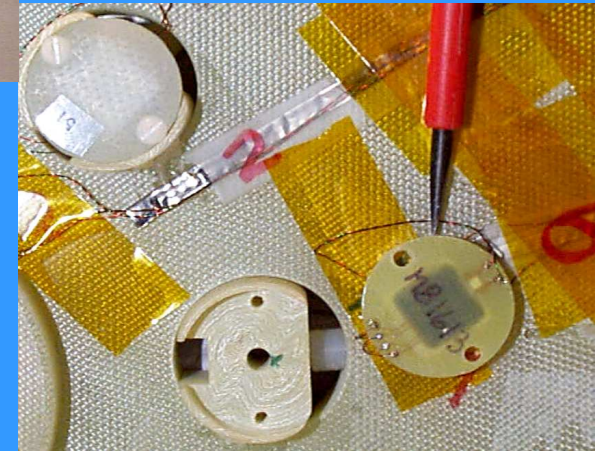
Superconducting
"helmet" made of
a thin lead sheet.



155 ch SQUID
array installed
inside
superconducting
imaging surface
"helmet"

Integrated
SQUID sensors
and pickup coils

A large array sensor for MEG
based on the superconducting
imaging surface gradiometer
concept.

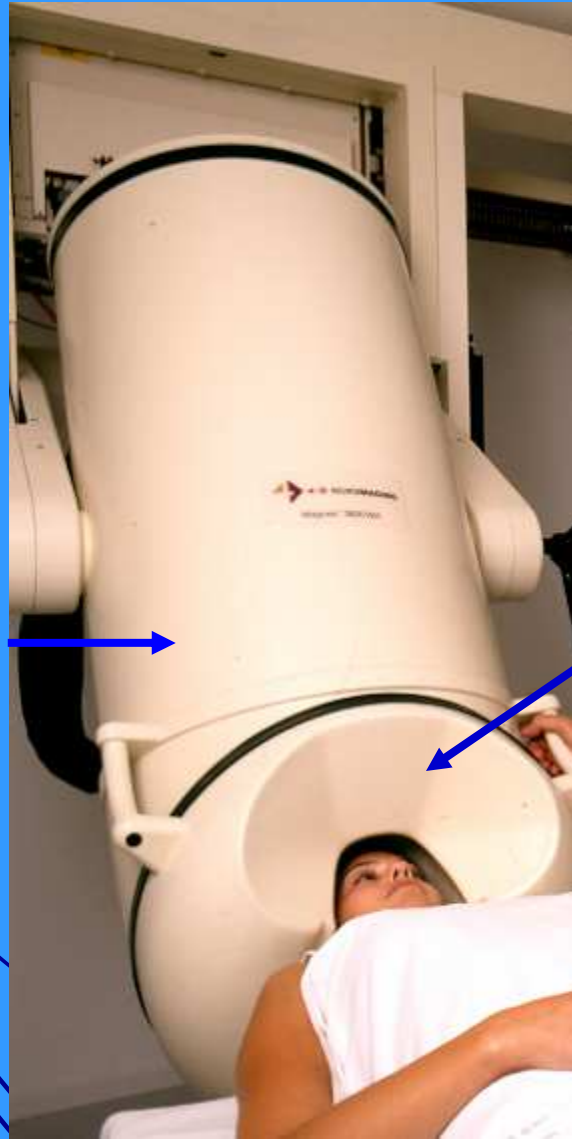


Senior Scientific

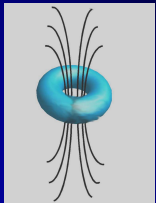


The University of New Mexico

The Dewar
Liquid helium



- 248 axial gradiometers (low noise)
- 1 kHz sampling rate



Senior Scientific

The MEG instrument at the Minneapolis Domenici Center
(Magnes 3600WH, 4-D Neuroimaging, San Diego, CA)



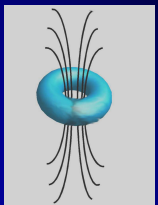
The University of New Mexico

MEG

Magnetoencephalography

Imaging the Brain

SpatioTemporal Analysis of
Sensor Magnetic Fields to
Image Brain Sources using
EM Inverse Solutions



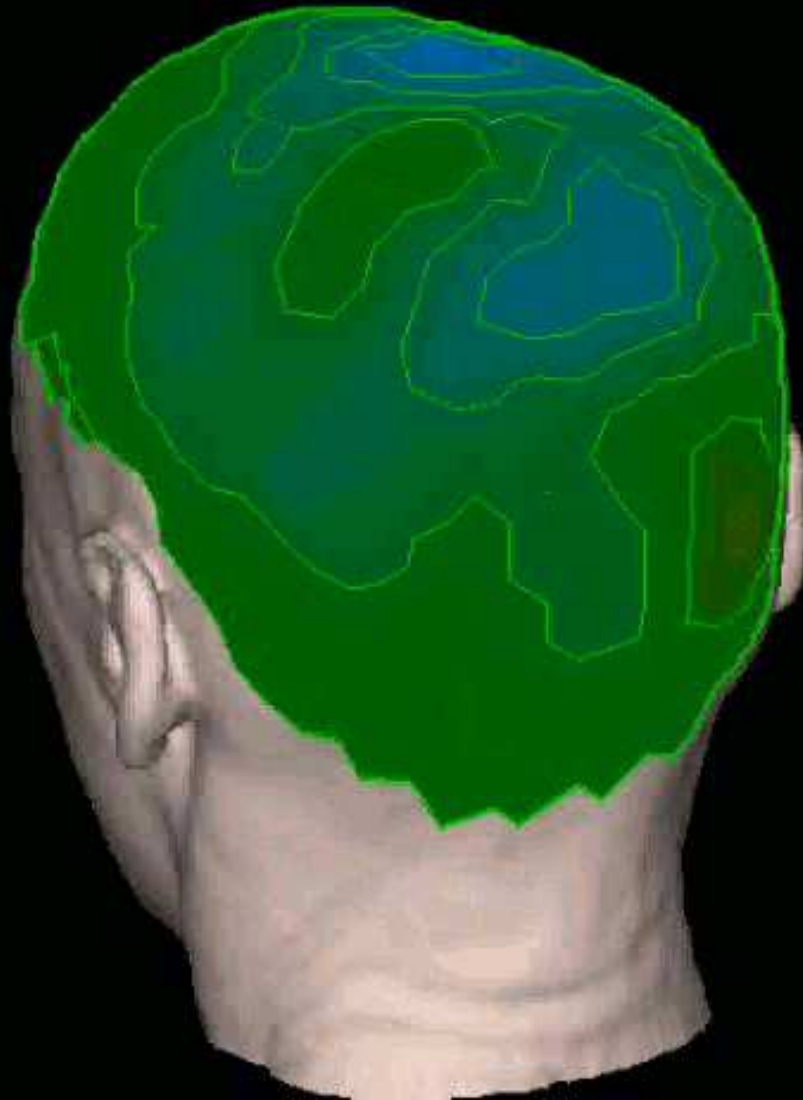
Senior Scientific



The University of New Mexico

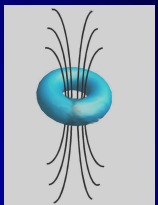
SQUIDS Measure Both Space and Time

milliseconds: 50



Magnetic field contour lines, plotted here as a function of time, are used to determine neural sources.

Response of the brain to a visual stimulus.

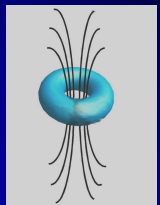
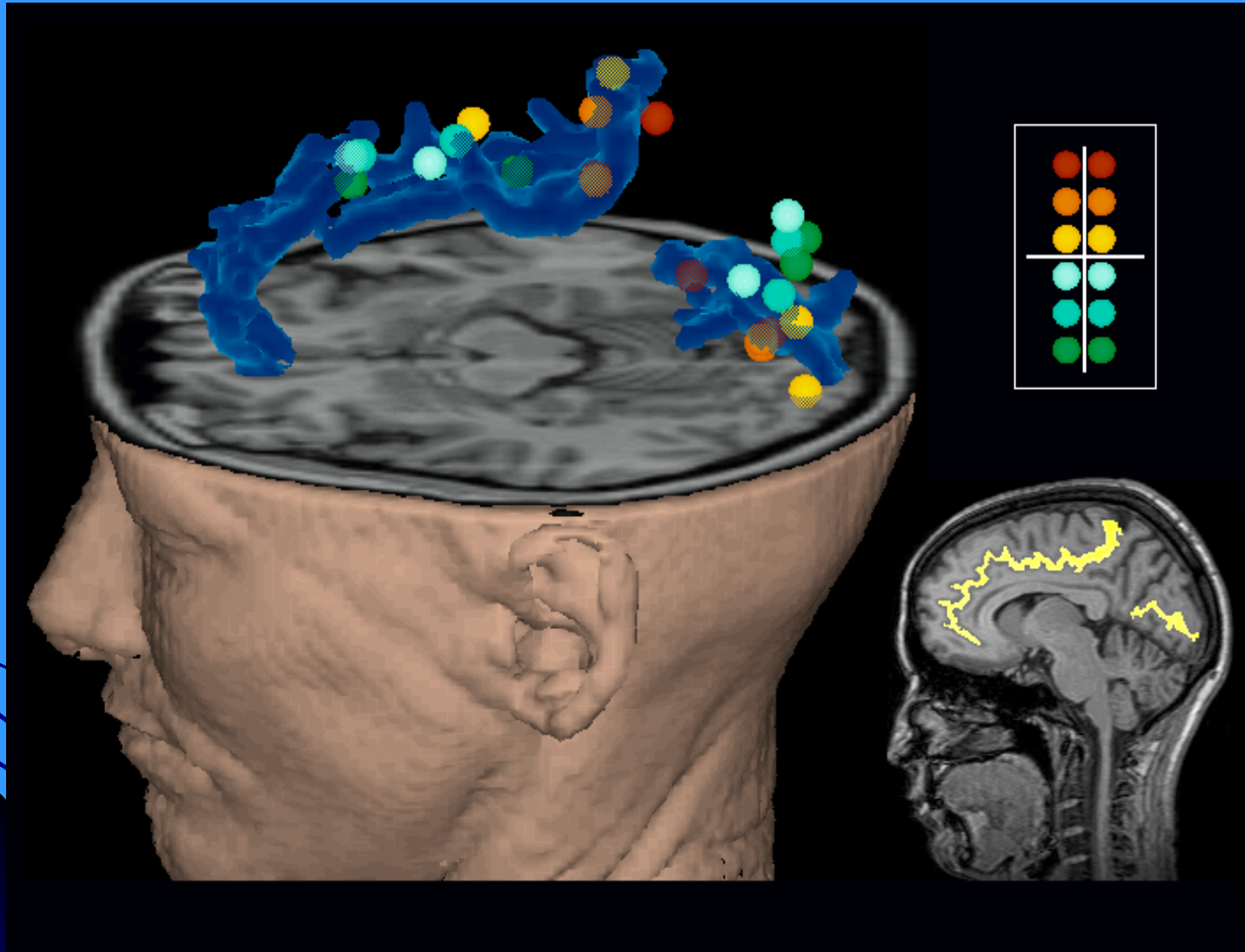


Senior Scientific



The University of New Mexico

Finding the Sources with a Spatial-Temporal algorithm



Senior Scientific

Graphics by
Ranken LANL

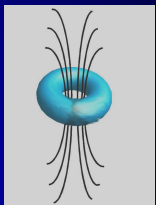


The University of New Mexico

MEG

Magnetoencephalography

Imaging the Mind
Examine correlations between
magnetic field magnitude and
time in sensor space
(No inverse problem)



Senior Scientific



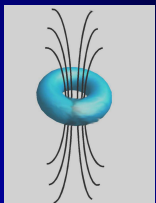
The University of New Mexico

Data Analysis - 1

Analyses are performed to estimate quantitatively the synchronous (i.e. zero-lag) interactions between signals from pairs of sensors to assess dynamic brain function.

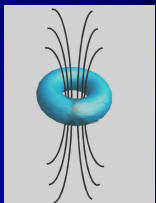
- **Step 1**: Calculate all pairwise zero-lag cross-correlations
- **Step 2**: Calculate the partial zero-lag cross-correlations within the 248-sensor network

Langheim, F.J.P., Leuthold, A.C. and Georgopoulos, A.P. (2006) Synchronous dynamic brain networks revealed by magnetoencephalography (MEG) Proceedings of the National Academy of Sciences USA 103: 455-459.

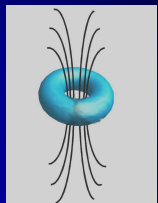
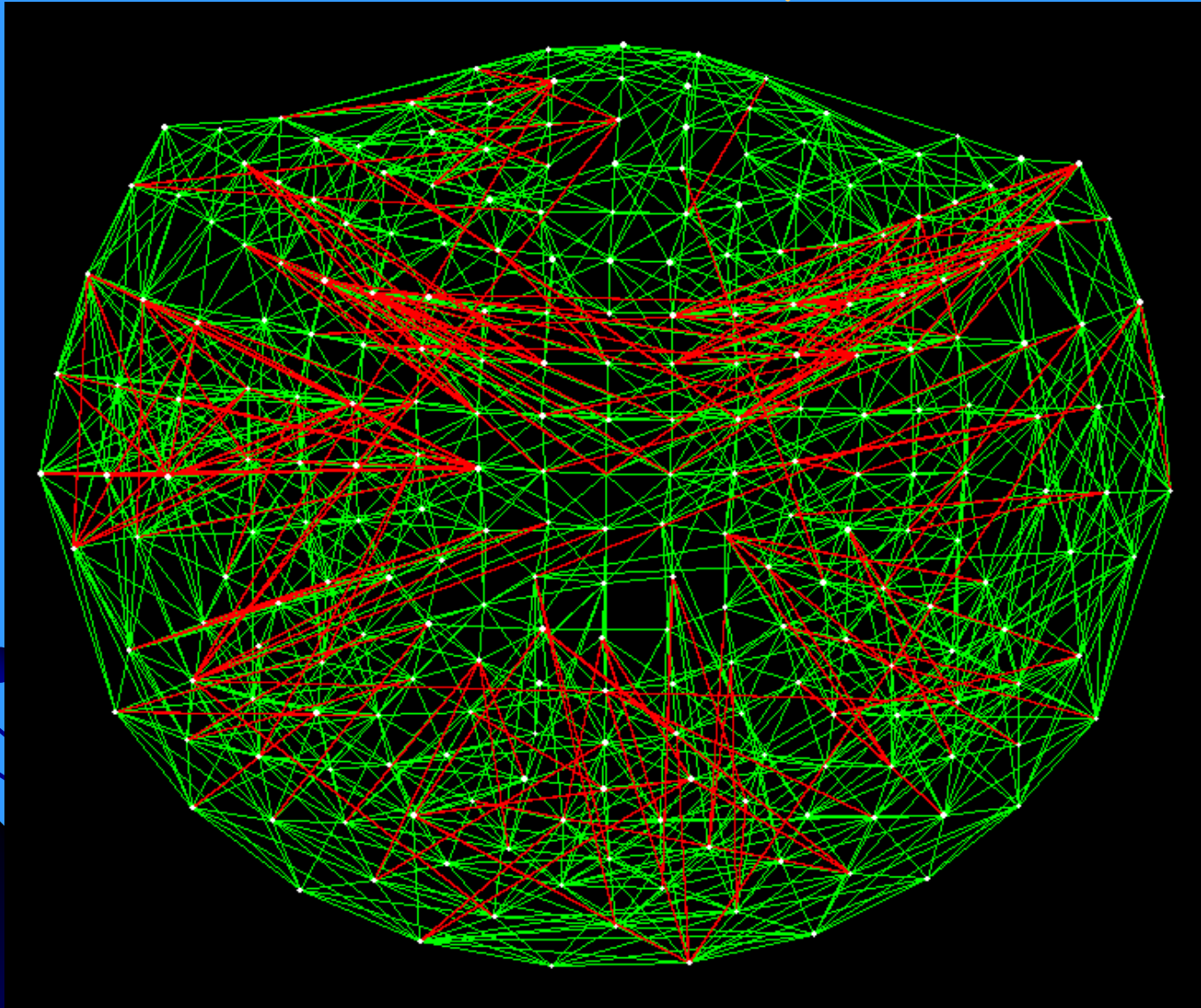


Data Analysis - 2

- The MEG time series are "prewhitened" by fitting an ARIMA (AutoRegressive Integrative Moving Average) Box-Jenkins model and taking the residuals
- This procedure yields practically stationary series from which CCF is estimated



Zero-lag (1-ms synchronous) Partial Correlations Of Prewhitened (stationary) MEG Time Series



Senior Scientific

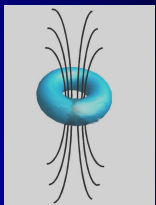
Langheim et al., PNAS, 2006



The University of New Mexico

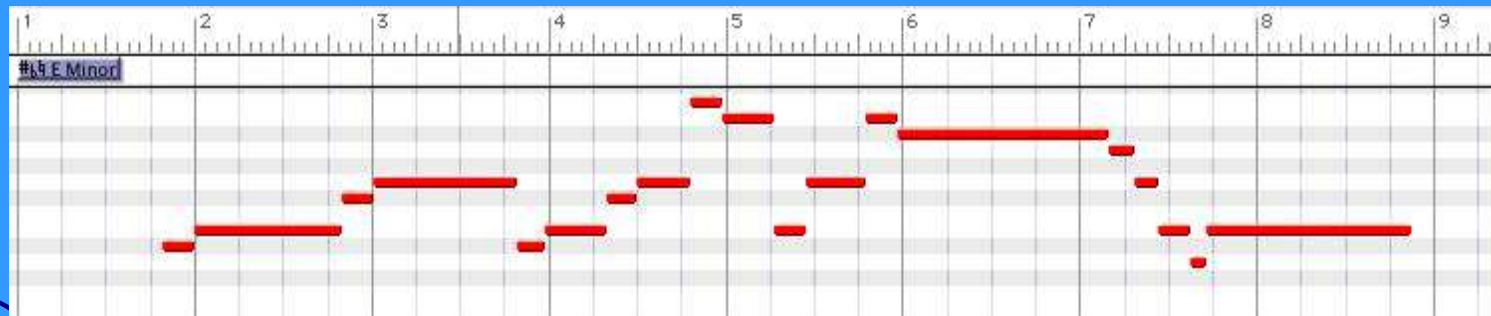
Predictions from raw MEG signals: Music Perception

- Subjects listened to a musical piece while MEG was recorded
- Single trials analyzed using multivariate regression of MEG data on MIDI notes of the piece
- Predicting MIDI notes listened to



Music Stimulus A

PPanther_Stimulus



Music Prediction A

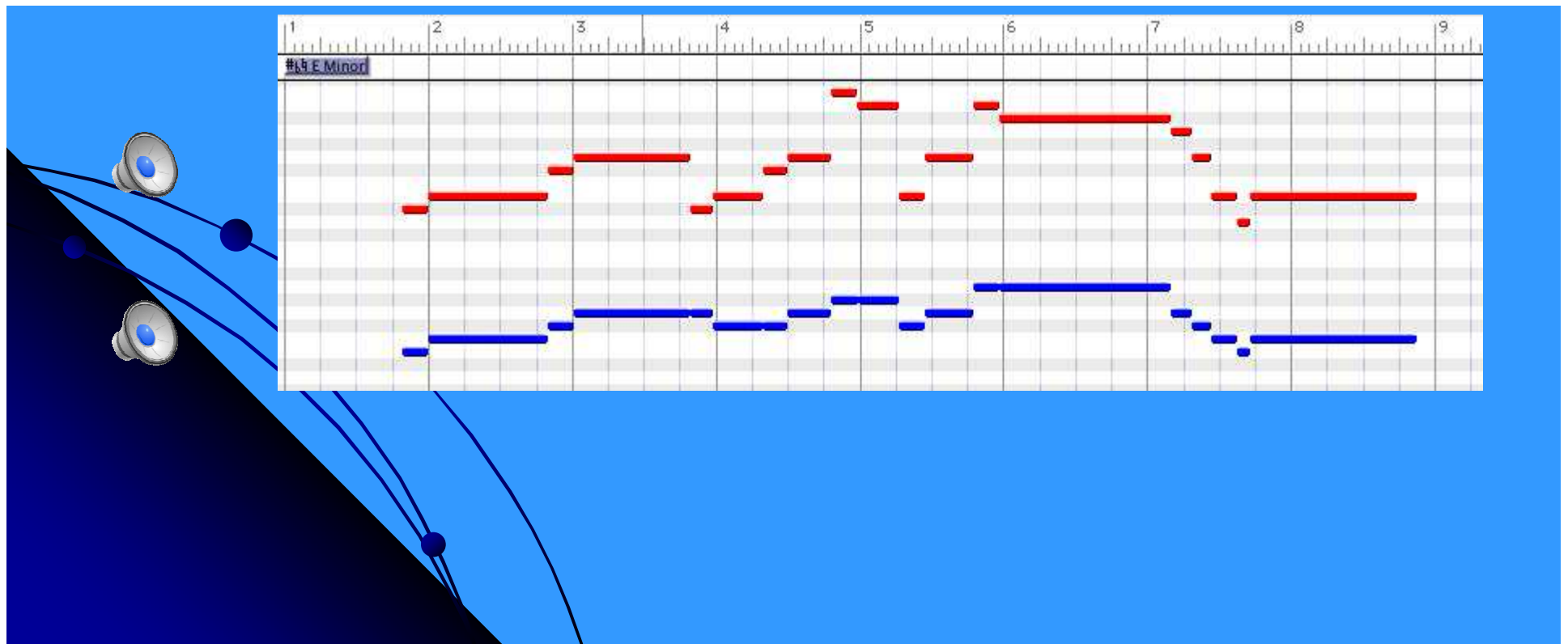
PPanther_Stimulus

PPanther_Prediction



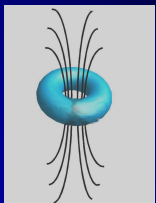
1 2 3 4 5 6 7 8 9

Detailed description: This block shows two staves of musical notation. The top staff, labeled 'PPanther_Stimulus', and the bottom staff, labeled 'PPanther_Prediction', both use a bass clef, a key signature of one sharp (F#), and a 4/4 time signature. The notation includes various note values, rests, and triplet markings (indicated by a '3' over a group of notes). The two staves are nearly identical, indicating a high level of prediction accuracy. Below the staves, a horizontal axis is numbered from 1 to 9, corresponding to the measures of the music.



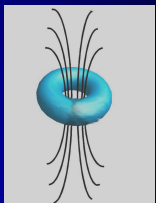
Assessment of Dynamic Brain Function: Synchronous Neural Networks

- Examine correlations between magnetic field magnitude and time in sensor space
- All possible zero-lag partial cross-correlations between 248 sensors (= 30,628)
- Positive or negative
- 1-ms temporal resolution = true synchronicity
- Simple fixation - look at a dot for 45 - 60 sec

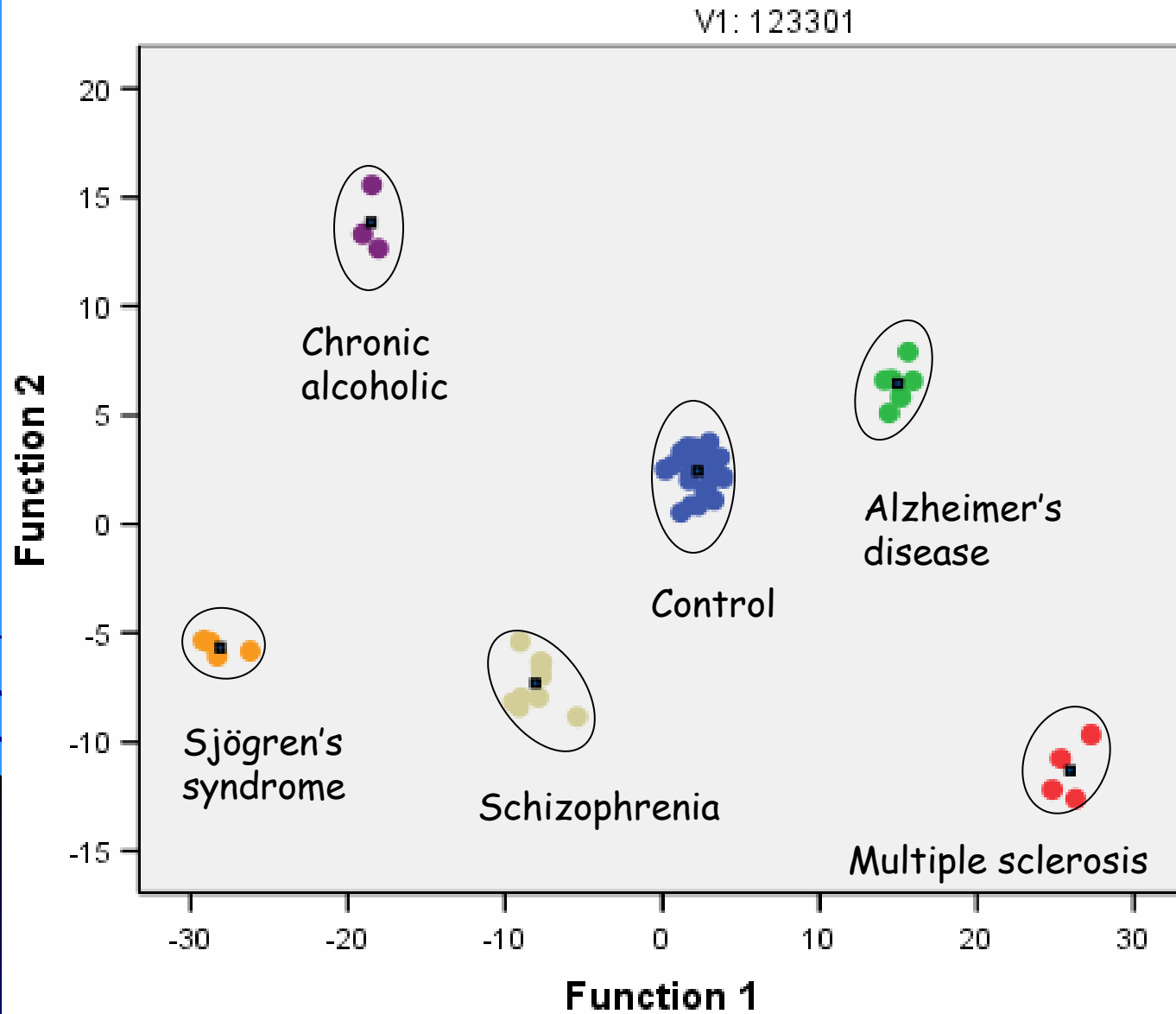


Discriminant classification analysis

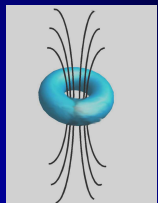
- Linear discriminant analysis
- Robust, cross-validated leave-one-out method
- 100% correct classification of 52 subjects to one of 6 groups (healthy control, Alzheimer's Disease, schizophrenia, chronic alcoholic, multiple sclerosis, Sjögren's syndrome) using as few as 10 zero-lag cross-correlations as predictors!
- Such sets are found in numbers far in excess of those expected by chance



Canonical Discriminant Functions



40 predictors



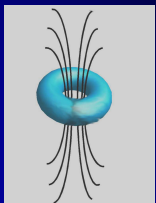
Senior Scientific



The University of New Mexico

Superparamagnetic Particles and the Detection and Imaging of Disease using Magnetic Sensors

Superparamagnetism



Senior Scientific



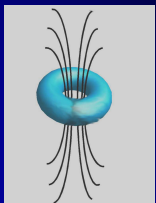
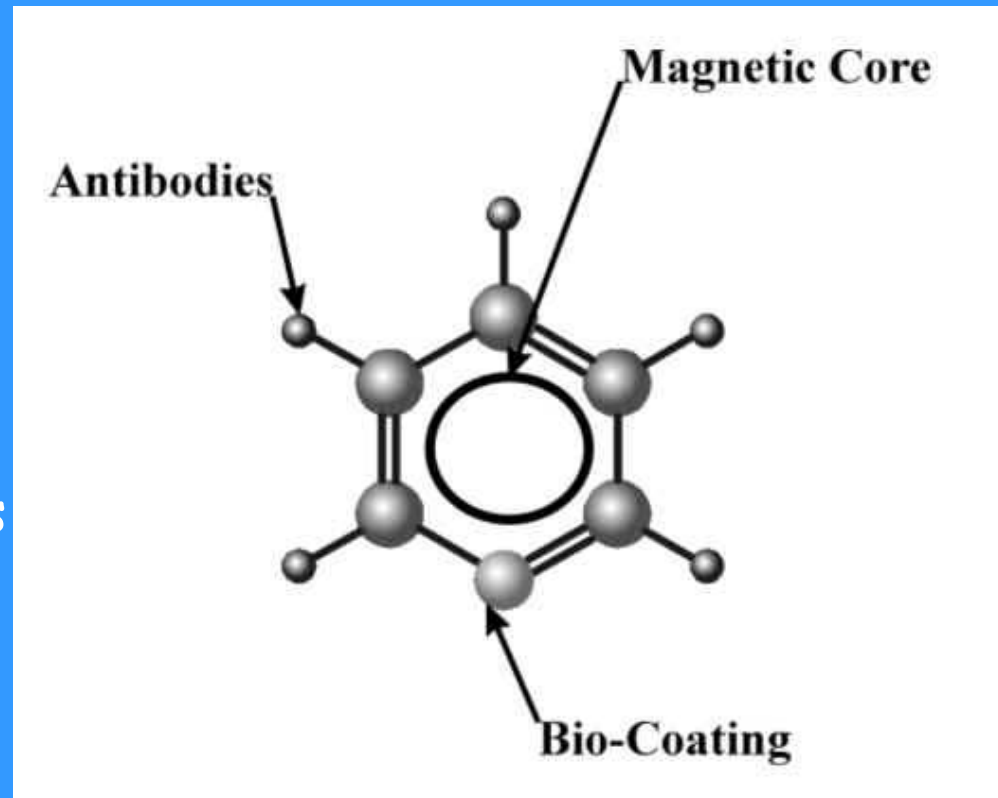
The University of New Mexico

Magnetic Nanoparticle with antibody attached

Typical magnetic core diameter is 20 -30 nm.

Typical bio-coatings are:
Carboxyl, starch,
streptavidin, PEG

Antibodies are specific markers for various types of cells; e.g., T-cells, various types of cancer cells, etc.



Superparamagnetism

Iron-oxide nanoparticles <100 nm diameter

Particles consist of a single magnetic domain.

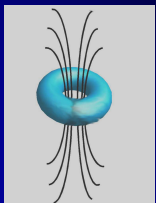
All internal atomic magnetic moments are aligned
(homogeneous magnetization)

Free particles randomize quickly by Brownian Motion

Bound particles decay by Néel Mechanism

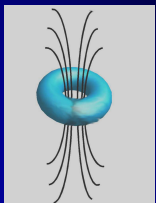
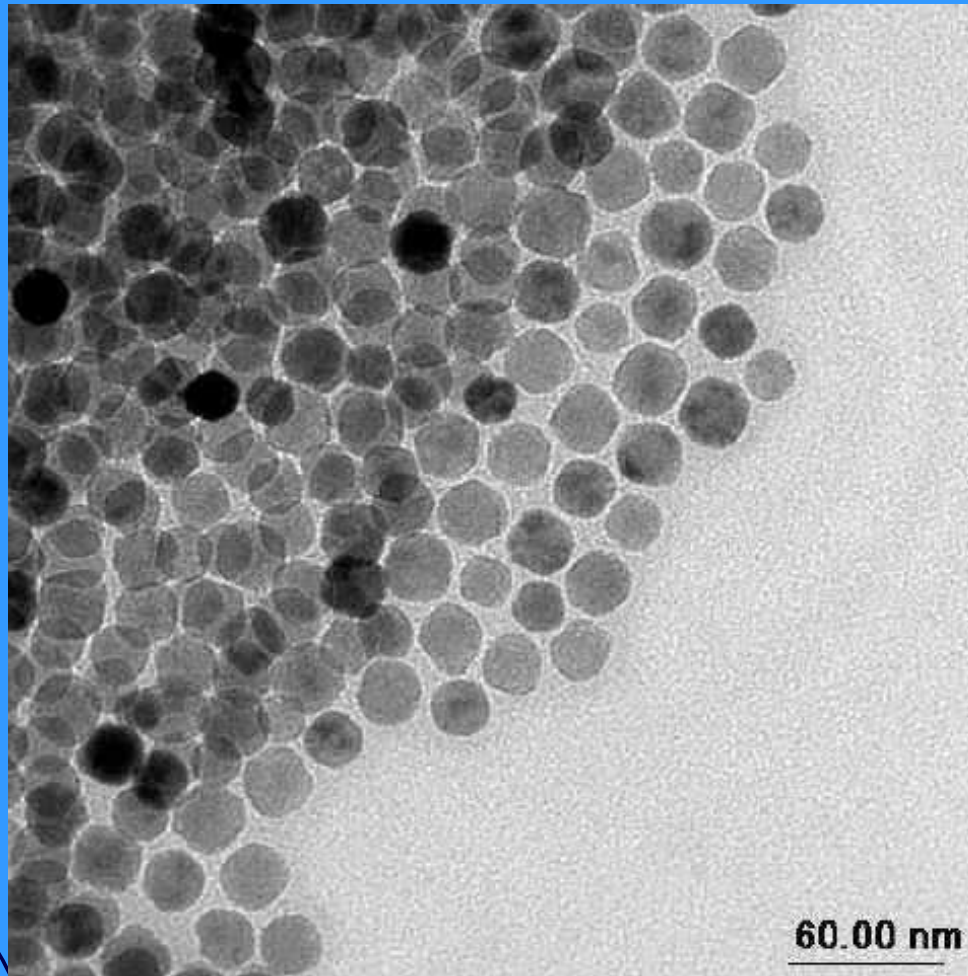
Particles exhibit large magnetic moments when magnetized

Particles behave as paramagnetic when not magnetized
(they do not agglomerate)



Scanning Electron Microscope View of Nanoparticles

Monodisperse magnetite 20 nm diameter, made at Center for Integrative Nanotechnology at Sandia National Laboratory (Dale Huber)



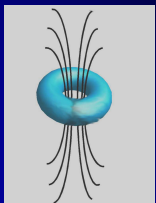
Senior Scientific



The University of New Mexico

Nanoparticles form a Magnetic Dipole when a magnetizing pulse is applied

- An induced collective dipole moment $\mu(t)$ is the result of alignment of a collection of N particles each with a moment μ_p by an external pulsed field B for a duration t_0 .
- $\mu(t)$ decays as the individual particle orientations relax, this is called the remanence time.



The interaction of a nanoparticle of magnetic moment μ with a magnetic field

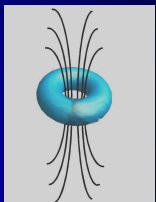
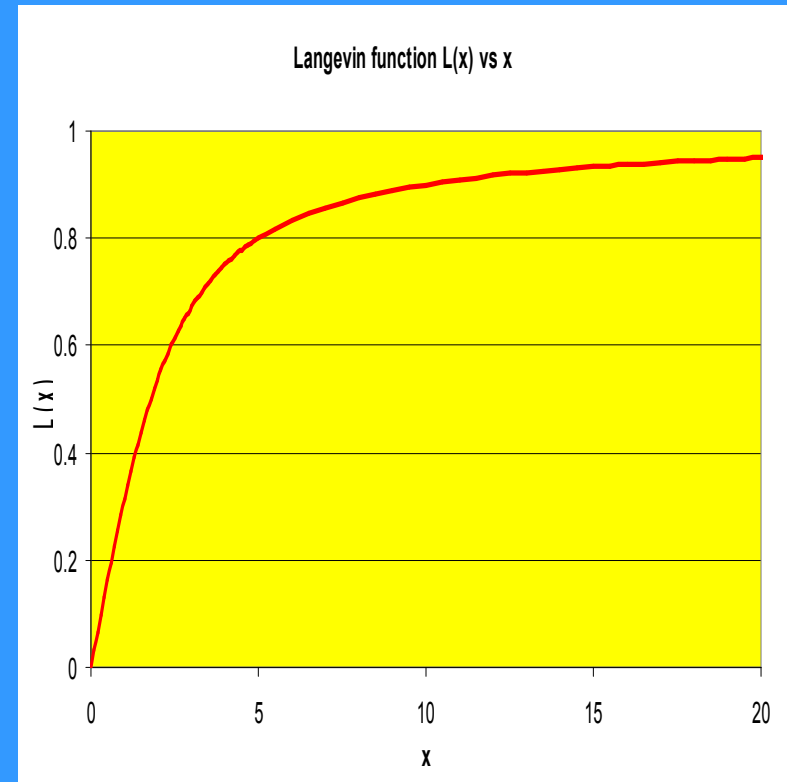
$$U = -\vec{\mu} \cdot \vec{B}$$

The average value of the cosine of the angle between is

$$\overline{\cos \theta} = \int e^{-U/kT} \cos \theta d\Omega / \int e^{-U/kT} d\Omega$$

The Langevin function, $L(x)$ gives the average value of $\cos \theta$ where $x = \mu B/kT$

$$L(x) = \coth(x) - 1/x$$



Senior Scientific



The University of New Mexico

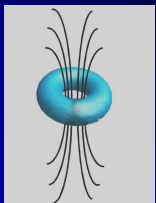
Dipole formed by the magnetic pulse and its decay

Each nanoparticle of radius r is aligned by the field of pulsed Helmholtz coils to form an initial moment determined by the Langevin function and the Néel relaxation time:

$$\mu_0(r, t_0, B) = \mu_p L(x) [1 - \exp(-t_0 / \tau(r, B))]$$

The decaying dipole seen by a SQUID is the sum of all the aligned nanoparticle moments as they randomize when the field is quenched.

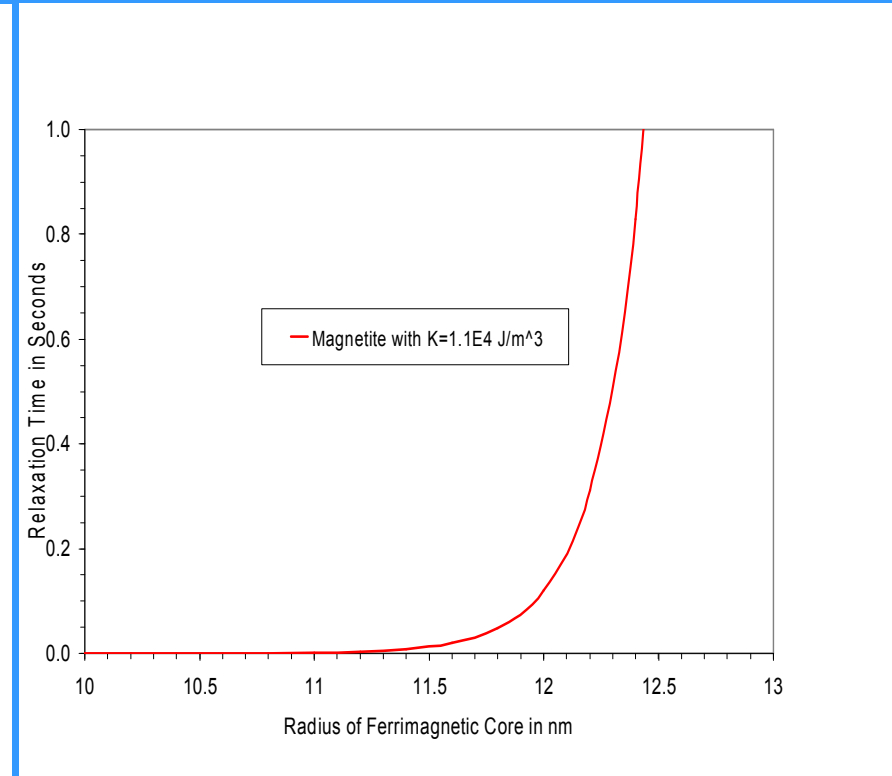
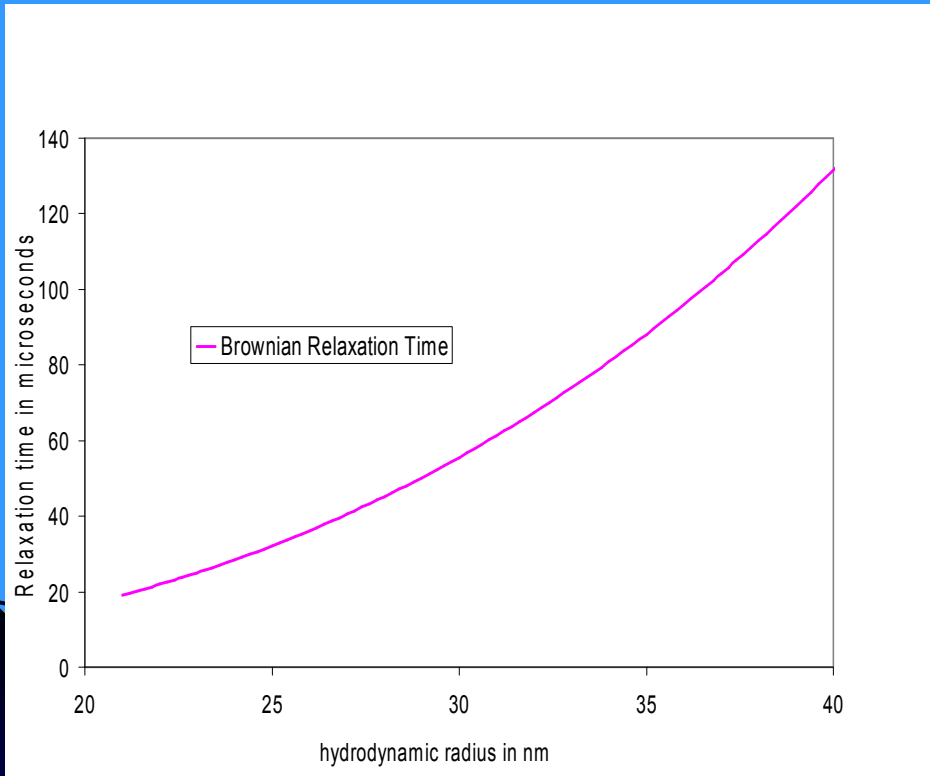
$$\mu(t, t_0, B) = N \int_0^{\infty} dr P(r) \mu_0(r, t_0, B) \exp(-t / \tau(r, 0))$$



Brownian vs Néel Relaxation Times

Free Particles

Bound Particles



Brownian

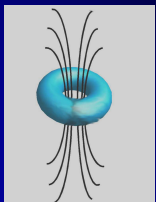
Néel

$$\tau_{Brownian} = 4\pi\eta R^3 / kT$$

$$\tau_{Neel} = \tau_0 \exp(KV / kT)$$

For polydisperse nanoparticles

$$B(t) = a_0 + a_1 * \ln(1+b/t)$$



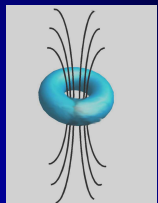
Senior Scientific



The University of New Mexico

Superparamagnetic Particles and the Detection and Imaging of Disease

Measuring the Remanence Fields



Senior Scientific



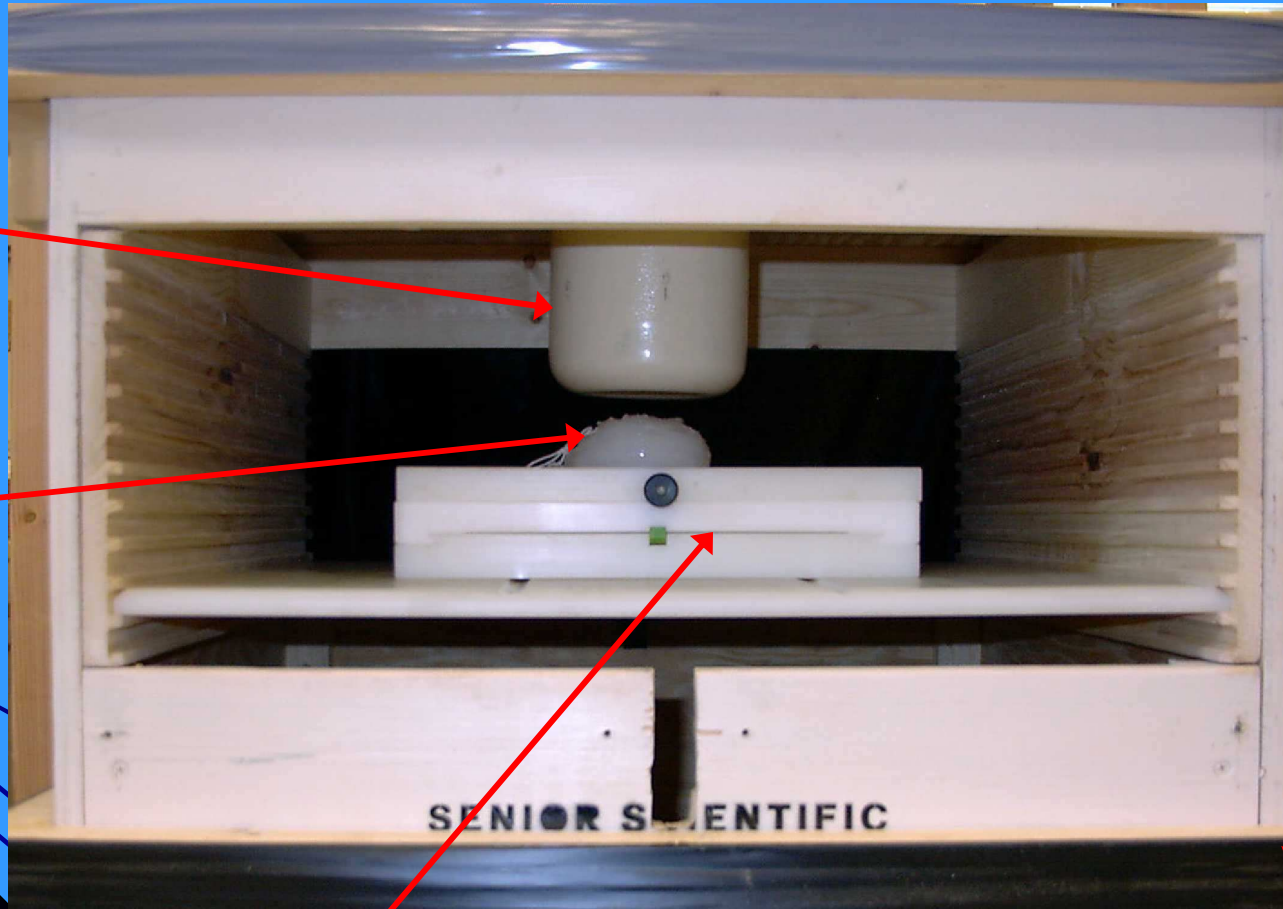
The University of New Mexico

7-Channel SQUID Measuring Chamber

SQUIDs

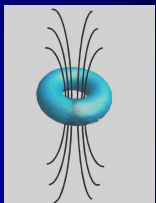
Cell Source

Helmholtz Coils

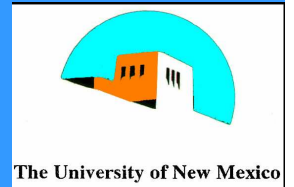


Non-Magnetic Stage

Multi-channel system permits vector moment measurements

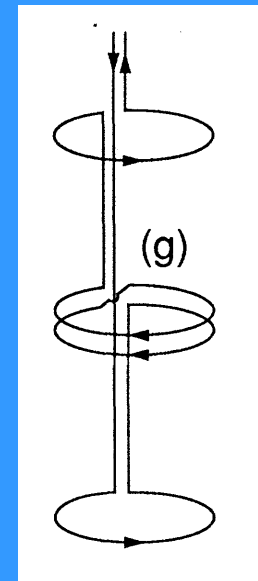
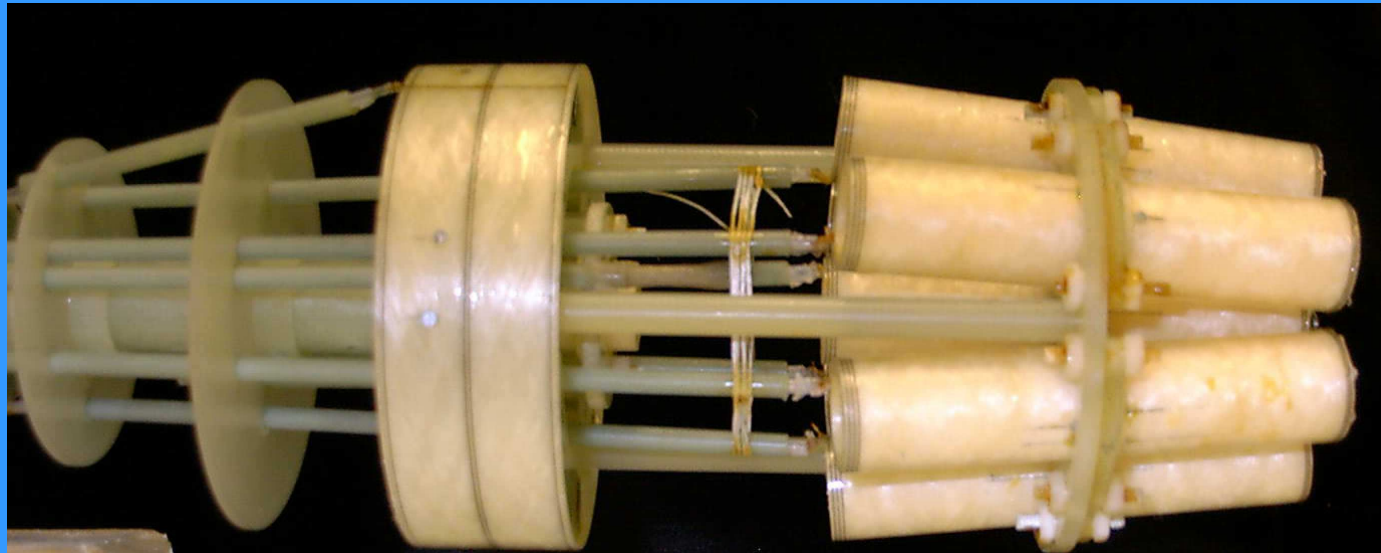


Senior Scientific

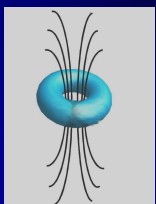


The University of New Mexico

Second-order gradiometer Sensor Array



Measures 2nd derivative of magnetic field to minimize background pickup of external fields. Permits operation without the need for a magnetically shielded room.



Senior Scientific

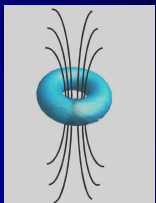


The University of New Mexico

Methodology

Procedure for Measuring Remanence Fields

- 1) Antibody-nanoparticles injected into subject ($< 1\text{mg Fe}$).
- 2) Subject placed under sensor system
- 3) Magnetizing pulse applied (38 Gauss applied for 0.30 sec)
- 4) Remanence fields measured for two Seconds
- 5) Magnetic moment and location of source(s) obtained
- 6) Number of detected cells determined



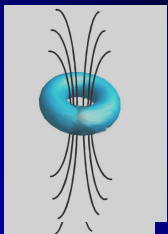
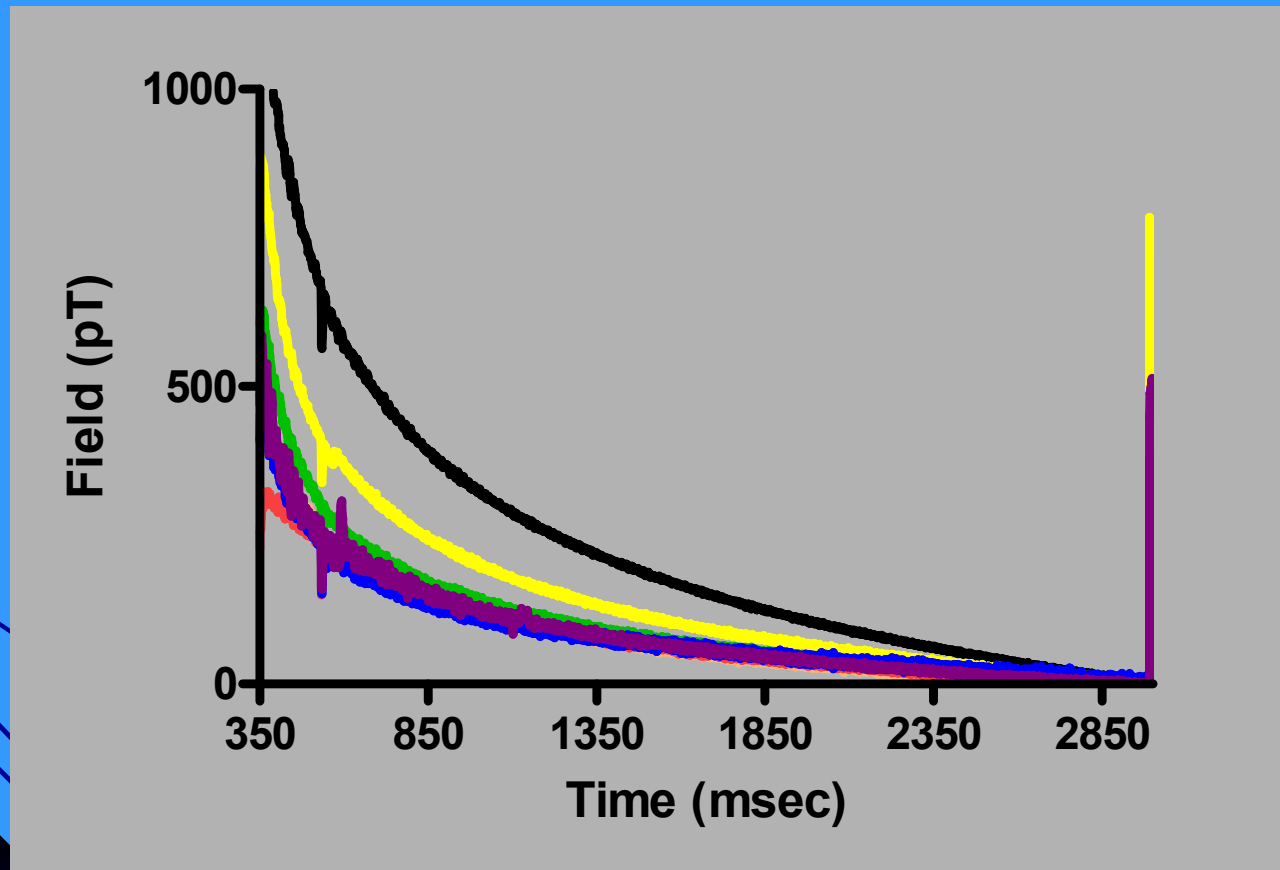
Senior Scientific

E R Flynn and H C Bryant, "A biomagnetic system for *in vivo* cancer imaging," *Physics in Medicine and Biology* 50 (2005) 1273-1293



The University of New Mexico

Example of 7-channel SQUID remanence fields



Senior Scientific

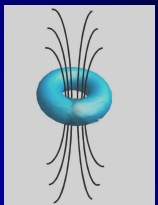


The University of New Mexico

Disease detection procedure

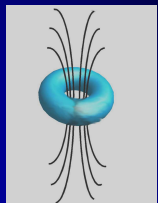
Calibrate Cell Sensitivity:

- Measure magnetic moment per particle by fitting magnetization curve to Langevin function
- Measure magnetic moment of cell sample with known number of cells
- Calculate number of nanoparticles/cell for each cell type



Superparamagnetic Particles and the Detection and Imaging of Disease

Detecting and Locating Cancer

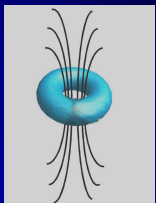
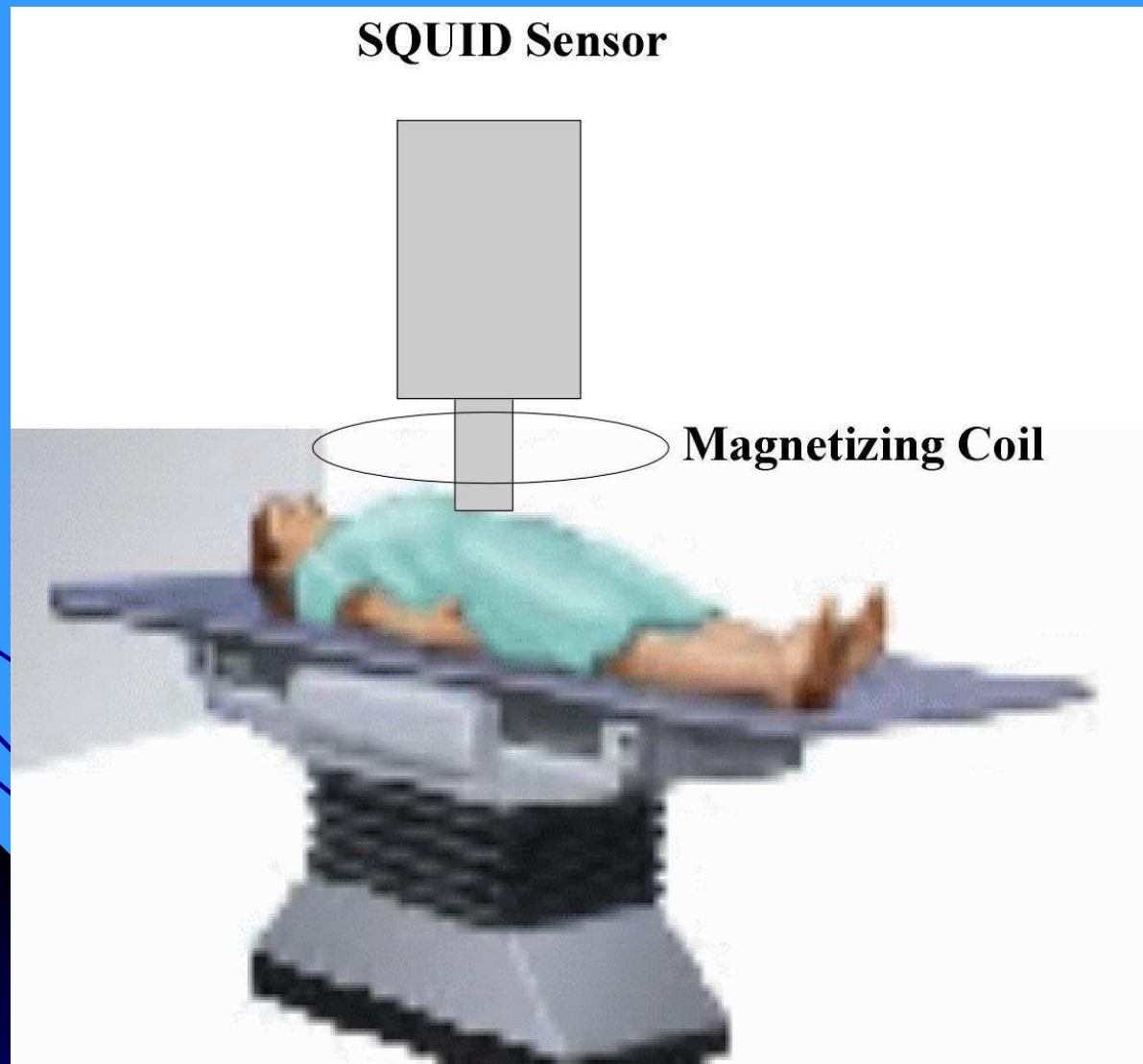


Senior Scientific

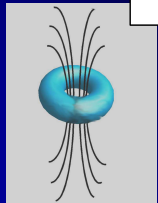
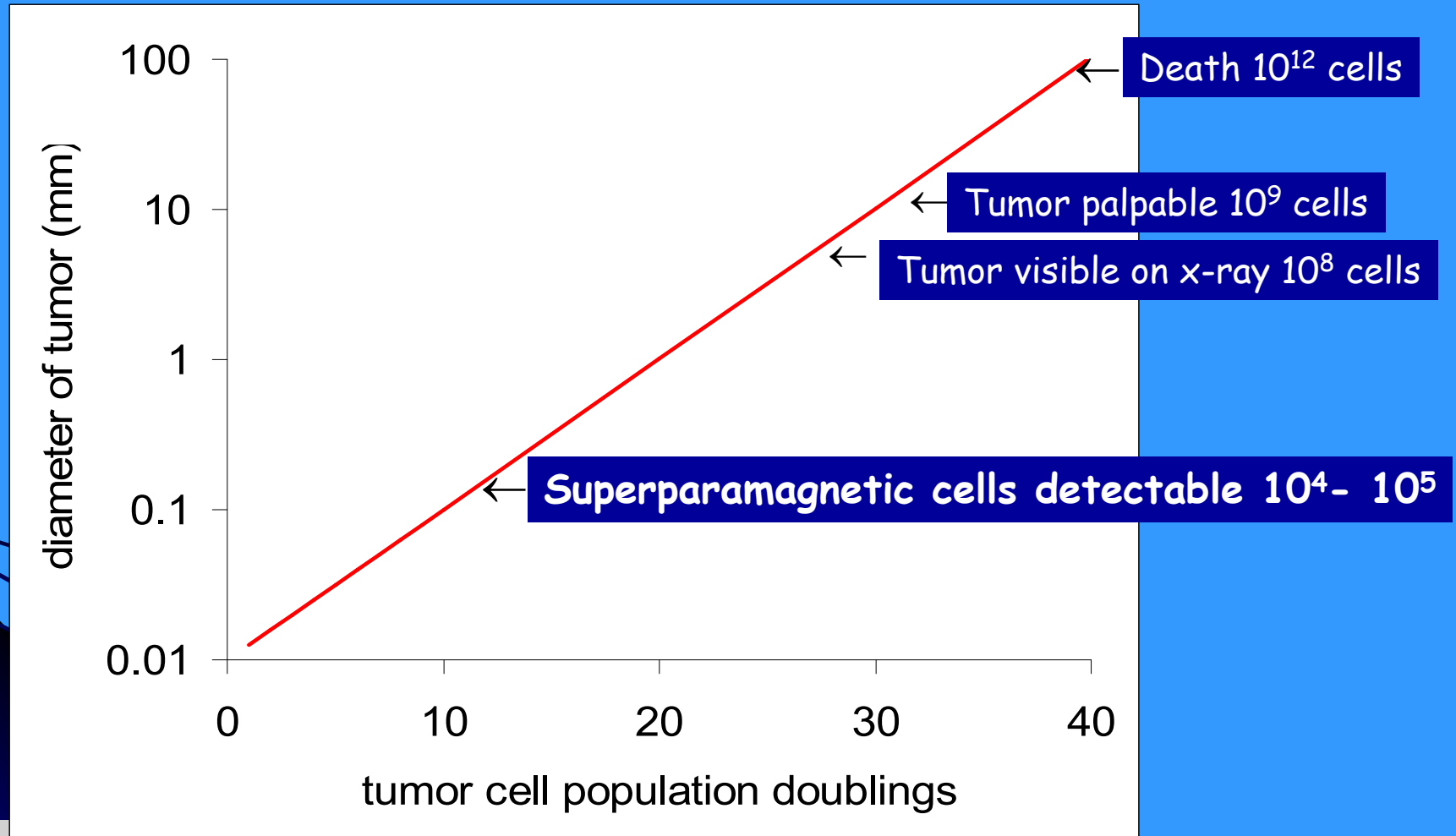


The University of New Mexico

Clinical Arrangement in unshielded environment



Growth of human tumor

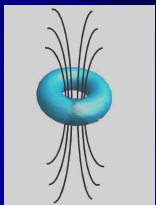


Breast Cancer

Breast Phantom
with two vials
of live breast
Cancer cells
(MCF-7)
Coupled to
Magnetic
nanoparticles with
HER-2 antibodies



Sensitivity for breast cancer
cells = 10^5 cells for depths up to
8 cm into breast. Imaging
accuracy is +/- 3 mm.



Senior Scientific

Breast Cancer Markers and Cell Lines currently under study

Antibodies:

HER-2 antibodies

CA27.29 Breast Tumor Marker present on epithelial cells and elevated in breast cancer (33% in early and 67% in late stage cancer)

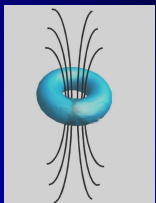
CA15-3 also elevated but not as specific

Angiogenesis:

VIP01 (vascular imaging peptide 01) binds to the integrin $\alpha_v\beta_3$ shown to be overexpressed at sites of neovascularization and metastasis.

Cell Lines Available:

BT-549, MDA-MB-436, MDA-MB-134-VI, HCC202, HCC1008, ZR-75-1, T-47D, MDA-MB-231, and BT-474.



Senior Scientific



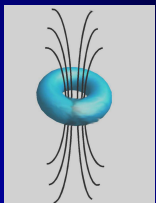
The University of New Mexico

Mouse Model of Human breast cancer

SCID Mouse with
human breast
cancer Xenograft
on flank.

MCF7 Cancer Cells

Mouse injected
with Nanoparticles
coupled to HER-2
antibodies



Senior Scientific



The University of New Mexico

Results of Mouse Tumor Study

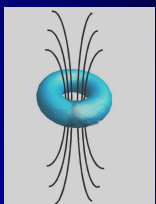
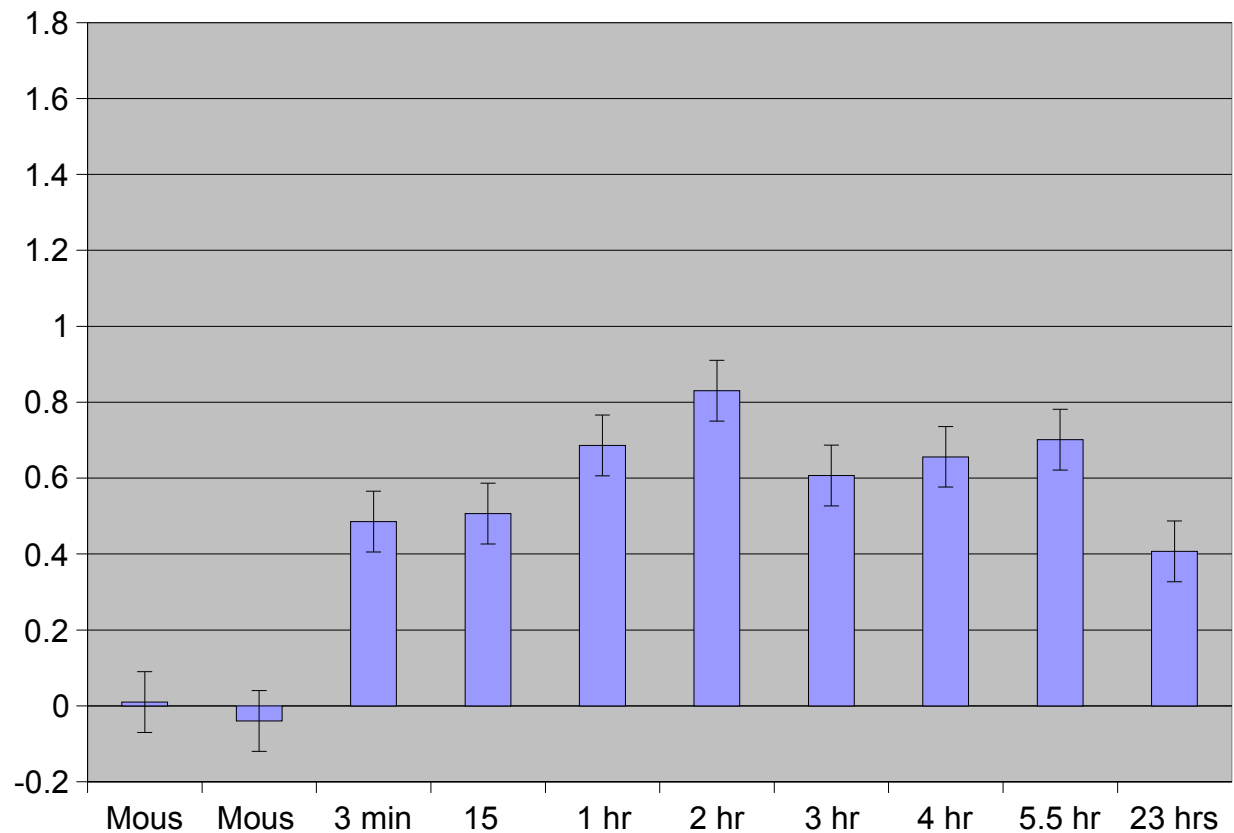
Magnetic moment
($\times 1E+07 \text{ A}\cdot\text{m}^2$)

as a function of
time from mouse
tumor after
injection of
nanoparticles.

$\mu = 1.0 = 2.6 \times 10^{10}$
nanoparticles =
 $\sim 3 \times 10^6$ cancer
cells

($\sim 1 \times 10^4$ np/cell)

Magnetic Signal from Mouse after Intratumoral injection



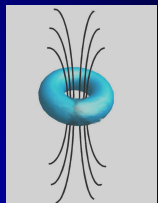
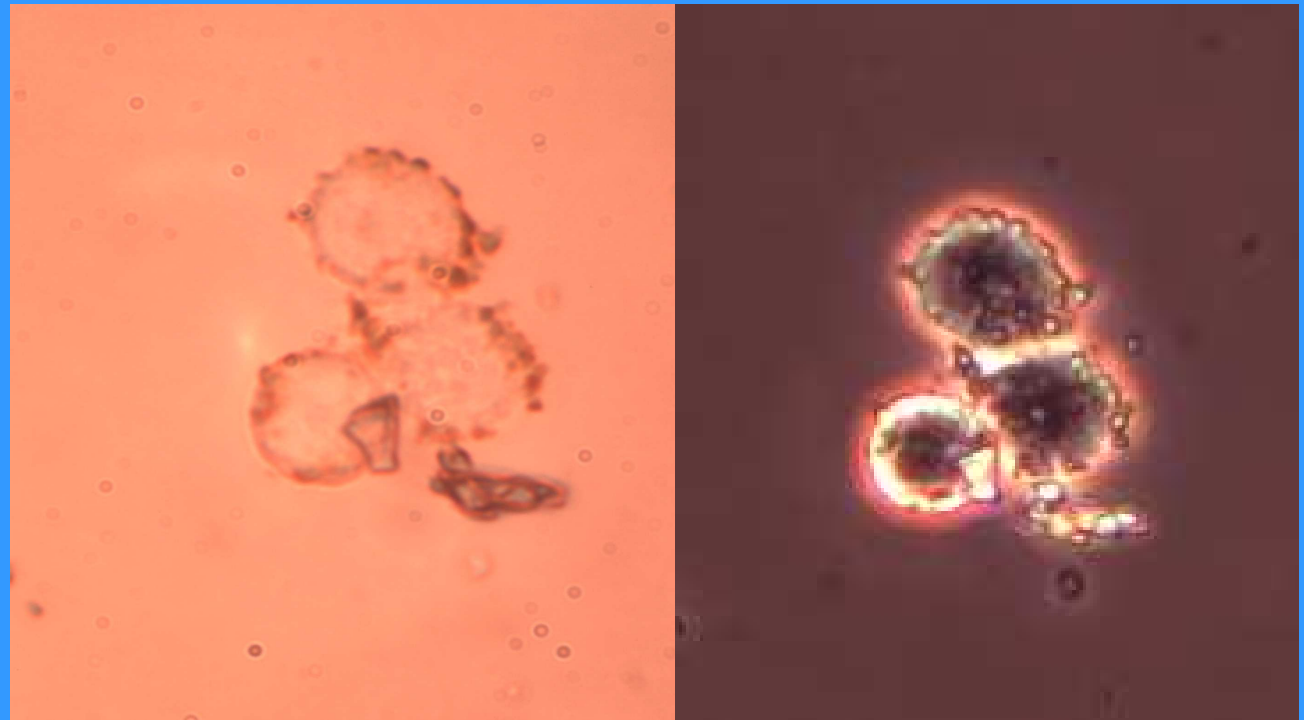
Senior Scientific



The University of New Mexico

Labeling of Breast Cancer Cells with magnetic NP

BT474 breast tumor cells, labeled with SiMag 1411 Carboxyl magnetic NP, coupled to anti-her2 Ab. Left is bright-field image of BT474 cells showing NP bound to surface, Right image is dark-field image.



Senior Scientific



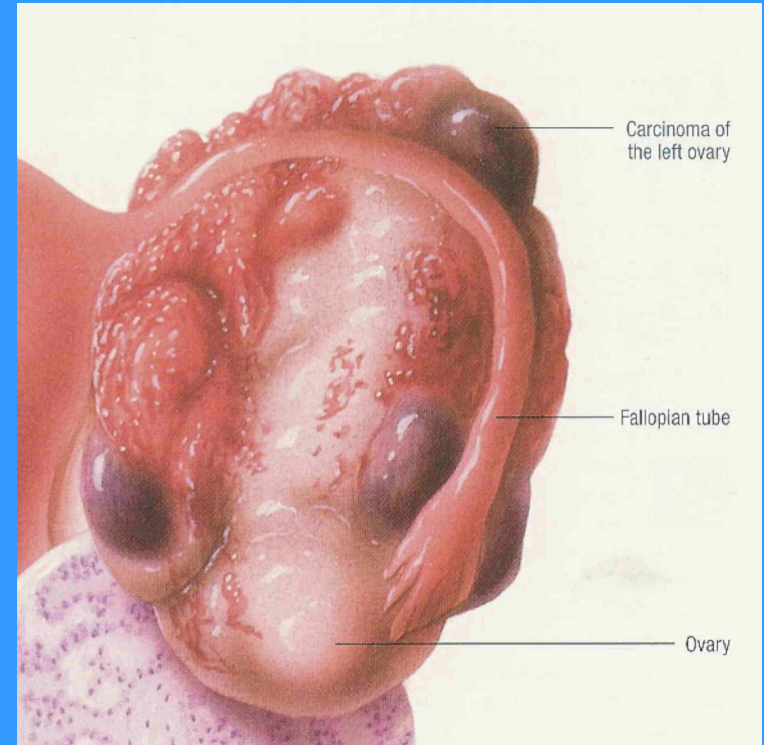
The University of New Mexico

Ovarian Cancer

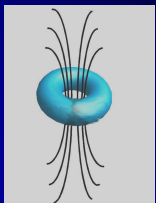
Anatomical Model under sensor system.



Ovary with Carcinomas



Nanoparticle in-vivo imaging permits several consecutive injections of different markers to improve sensitivity and specificity; e.g., CA125 & HMFG1/G2 give 95% sensitivity 93% specificity

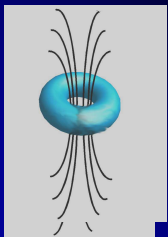
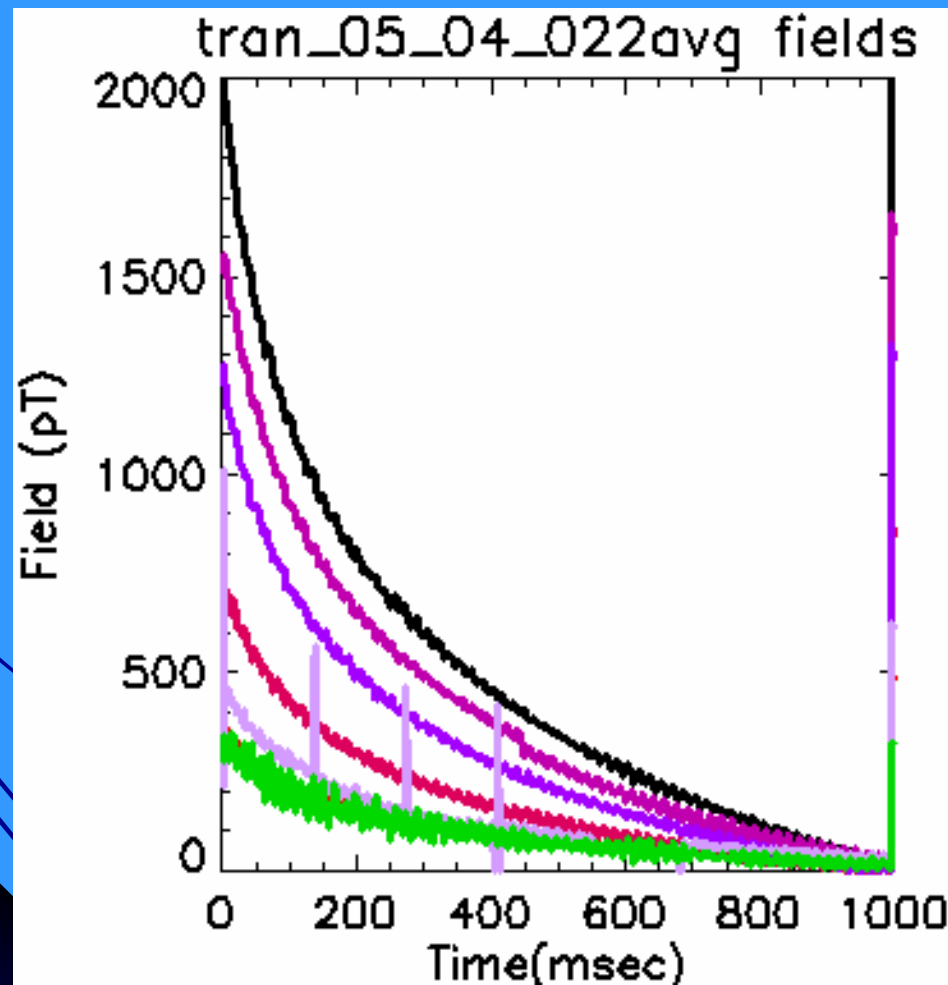


Senior Scientific



The University of New Mexico

7-channel SQUID remanence fields from 500,000 live ovarian cells coupled to nanoparticles with CA-125 markers.



Senior Scientific



The University of New Mexico

Live Ovarian Cell lines

Marker: CA125

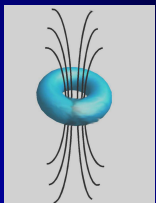
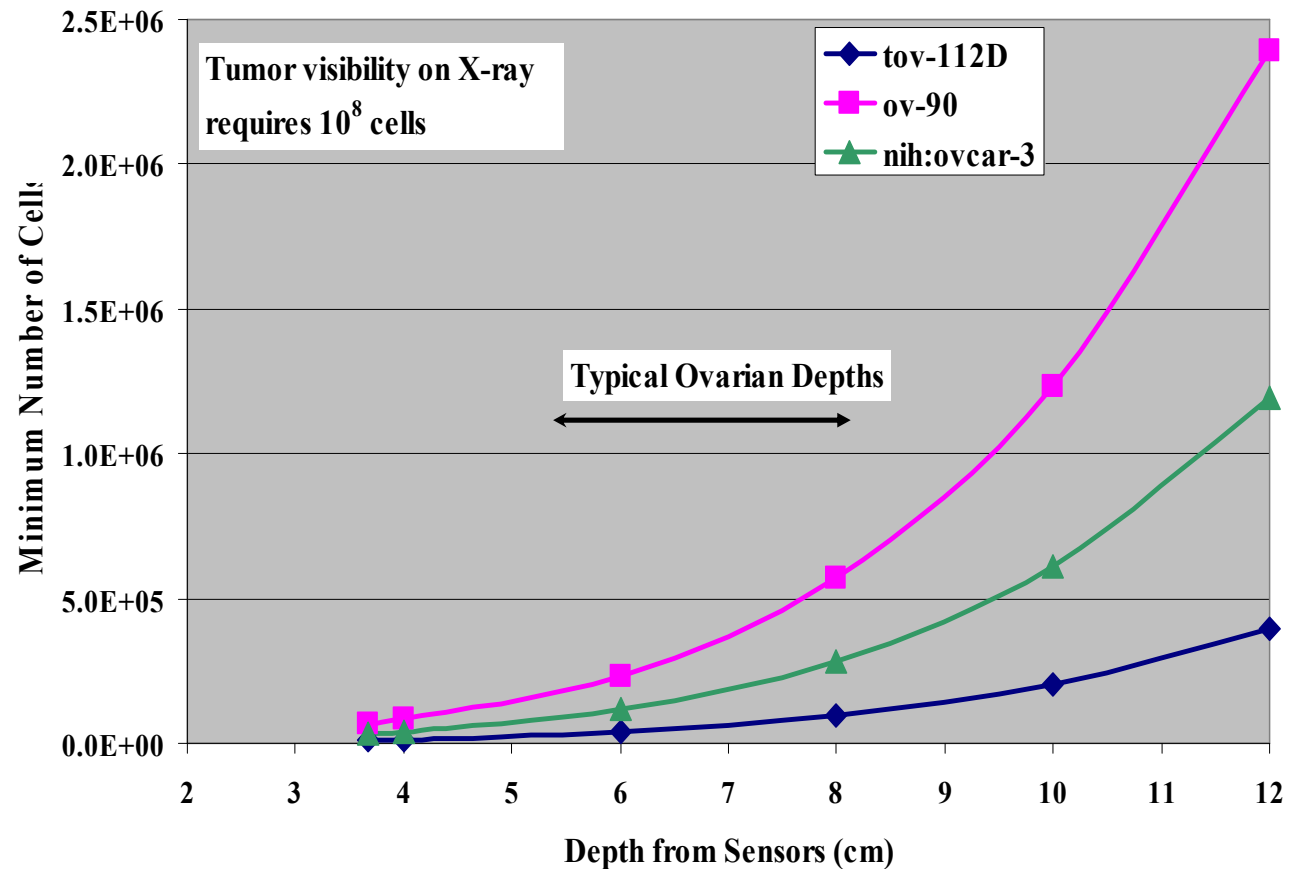
Cell Line NP/cell

tov-112D 2.04×10^4

ov-90 3.35×10^3

ovcar-3 6.73×10^3

Minimum Cells Detectable Vs Depth
for Three Ovarian Cell Lines (CA-125 Antibody)



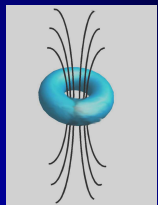
Senior Scientific



The University of New Mexico

Superparamagnetic Particles and the Detection and Imaging of Disease

Detecting Rejection of Transplanted Organ



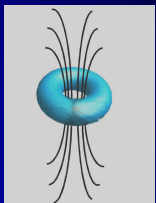
Senior Scientific



The University of New Mexico

In-Vivo Detection of the Rejection of a Transplanted Organ

- 1) Rejection of a transplanted organ occurs by T-cells that attach to foreign Human-Leukocyte-Associated antigens on the donor cells and kill them.
- 2) T-cells accumulate in small nodules within the organ.
- 3) T-cells can be targeted with specific antibodies, conjugated to magnetic nanoparticles, and detected in-vivo by SQUID sensors.
- 4) Method minimizes the need for painful biopsies.
- 5) Monitoring for T-cell presence will be used to determine the amount of anti-immune system drugs being administered.



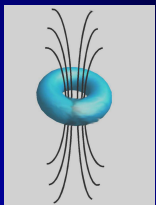
Senior Scientific



The University of New Mexico

Each T-cell will have 5×10^4 CD3 Antibodies conjugated to nanoparticles

- 1) Current SQUID system detects 10^5 cells at 4 cm and 10^6 at 8cm.
- 2) This corresponds to the amount in ~100 micron diameter nodules.
- 3) Completely rejected organ may contain $10^{10} - 10^{11}$ T-cells.
- 4) Transplanted organs include kidney, heart, liver and lung.



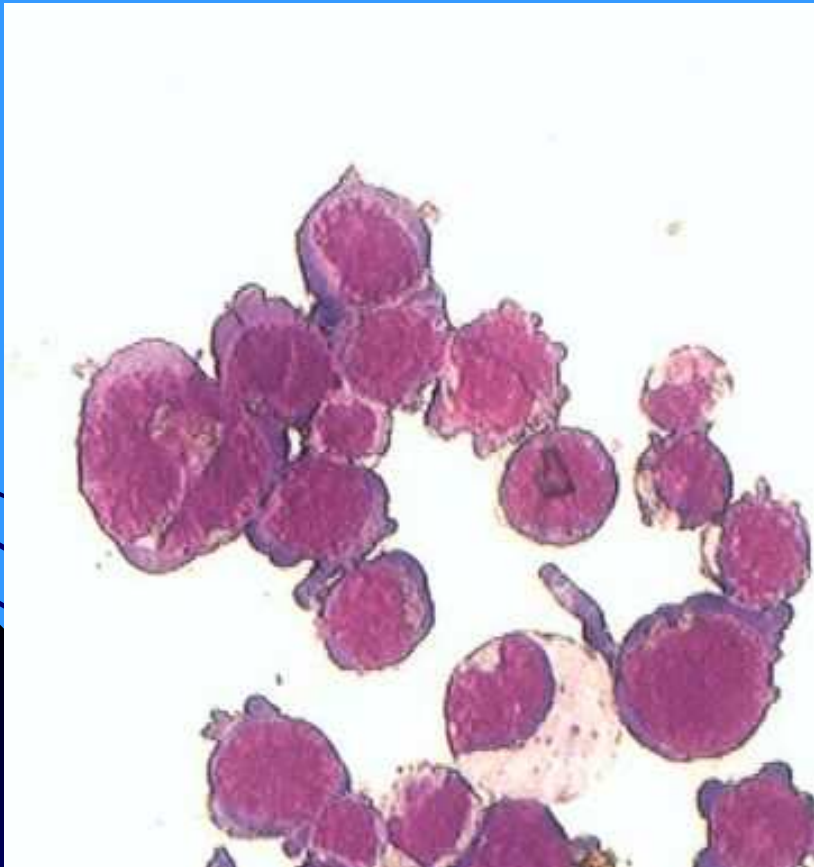
Senior Scientific



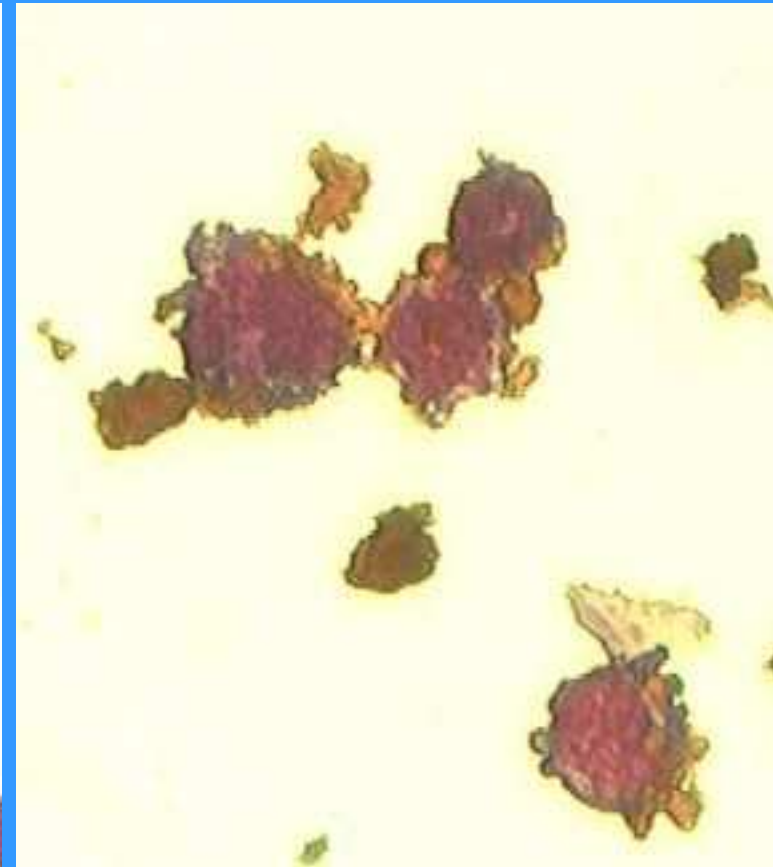
The University of New Mexico

Specific Binding of Nanoparticles to Cells

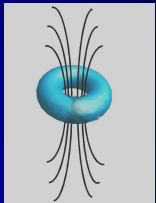
Jurkat T-Cells CD2 Antibody
(non-specific)



Jurkat T-Cells +CD3 Antibody
(specific)



Jurkat cells are leukemia T-cells

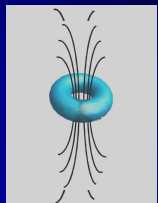
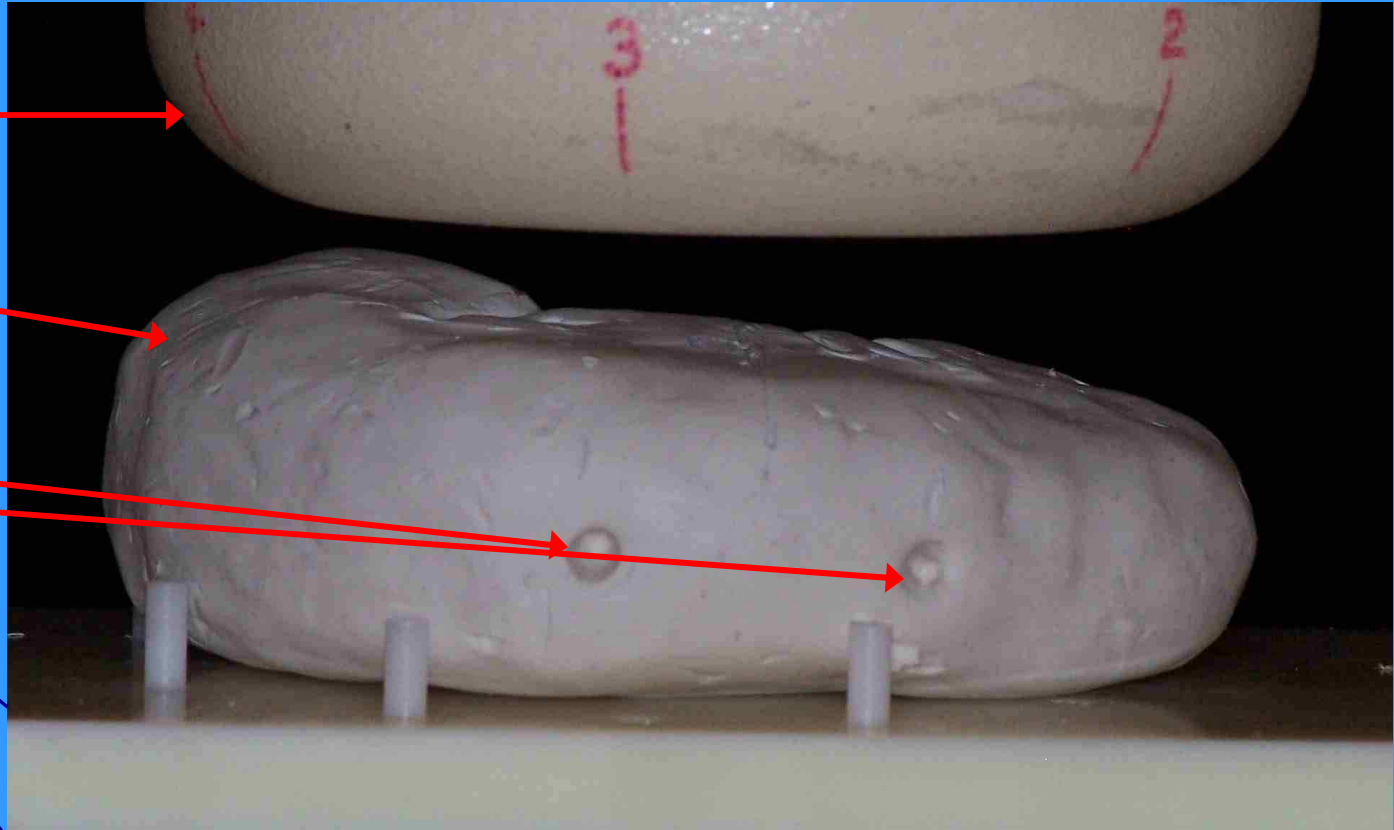


Kidney Phantom containing two sources of Live Jurkat T-cells under SQUID sensor

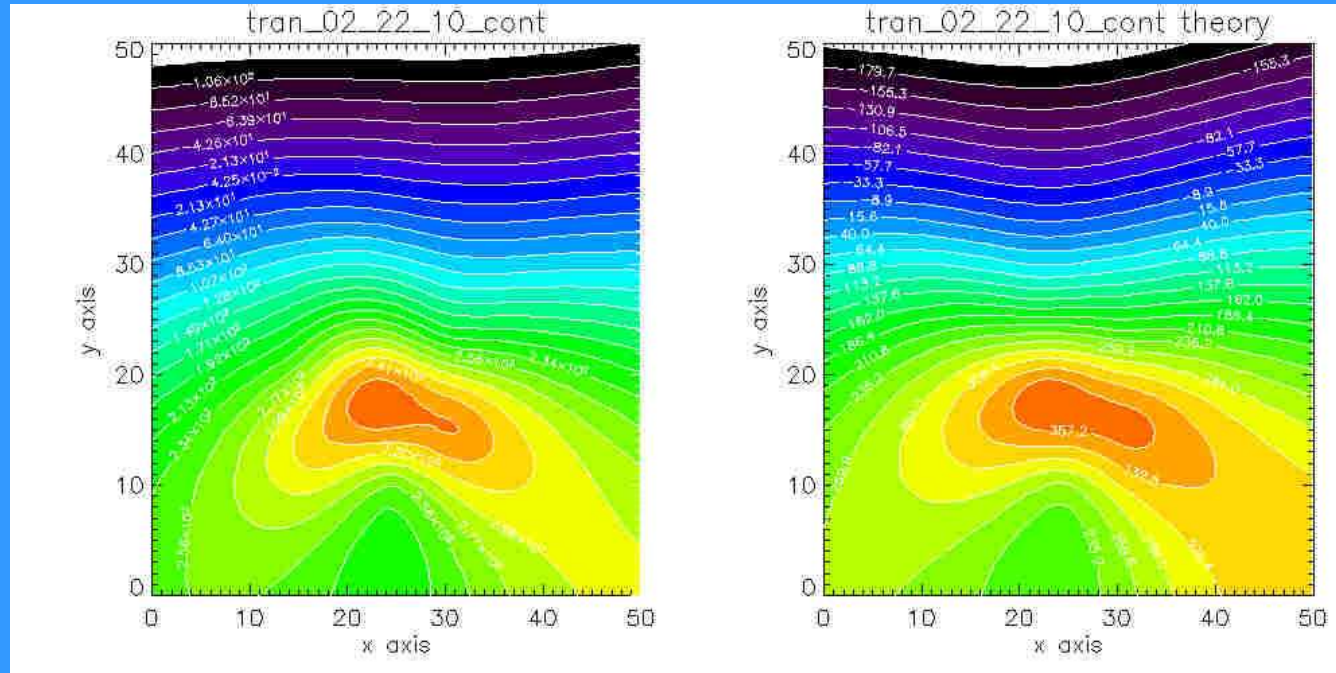
Sensor

Kidney

T-cells



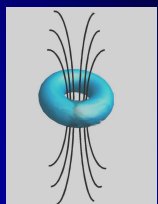
Magnetic Field Contours of Data and Theory for two Live Cell Sources in Kidney Phantom



Data Contours

Theory Contours

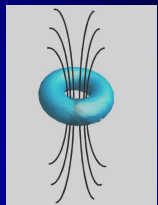
Source	x	y	z	m(A-m ²)	Cells
Source 1					
measured	1.4±.3	-1.1±.3	5.5±.3	1.52E-07	4.3E+06
imaged	1.3±.4	-1.9±.4	5.0±.3	1.45E-07	4.1E+06
Source 2					
measured	-2.7±.3	-1.5±.3	5.5±.3	1.60E-07	4.6E+06
imaged	-2.7±.4	-2.2±.3	5.0±.3	1.60E-07	4.6E+06



Senior Scientific

Superparamagnetic Particles and the Detection and Imaging of Disease

Diseases of the Brain



Senior Scientific

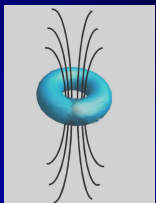
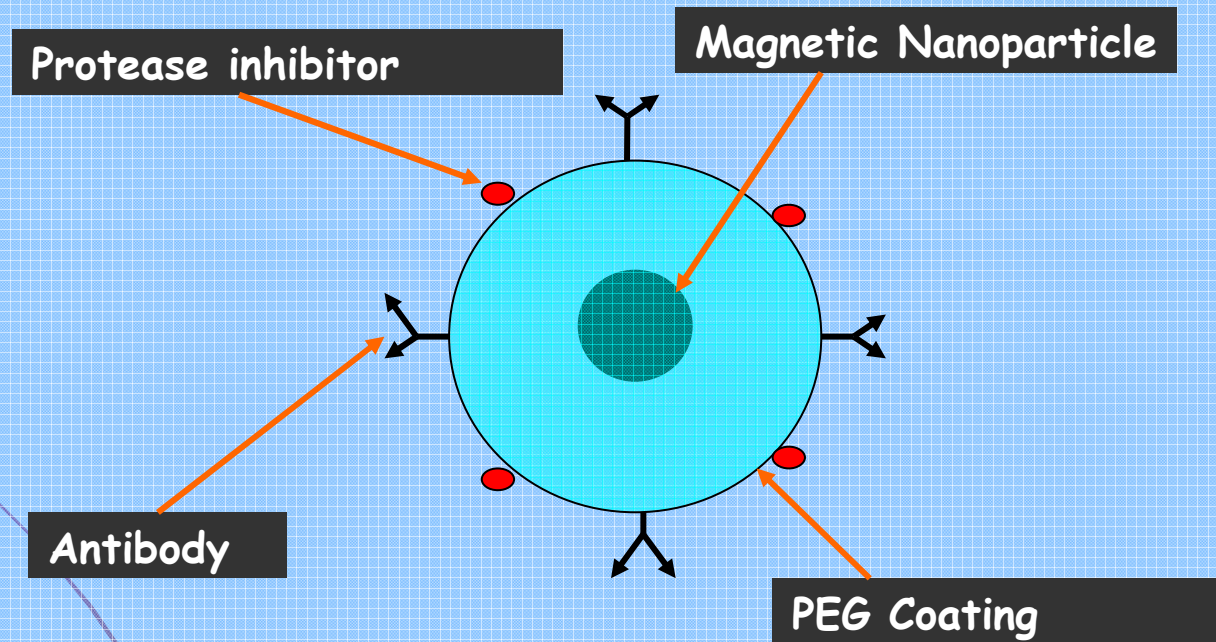


The University of New Mexico

Diseases of the Brain

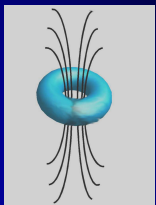
Nanoparticles and SQUID detection can be used to detect, and potentially treat, disease's of the brain; e.g., Alzheimer's and Multiple Sclerosis.

Specific coatings such as PEG help to get past the BBB with magnetic nanoparticles carrying Antibodies and Drugs



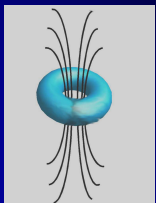
Methodology of Detection and Treatment of AD

- 1) Use nanoparticles coated with PEG to get by BBB
- 2) Use antibodies for Amyloid Plaque and Tau
- 3) Inject into patient and detect and localize plaque and Tau deposits
- 4) Determine presence and state of AD
- 5) Inject nanoparticles with antibodies and anti-plaque drug
- 6) Magnetically concentrate particles over localized plaque sites



Measuring Sources in the Brain

Model of brain placed in skull with multiple diffuse nanoparticle sources to measure multiple extended sources



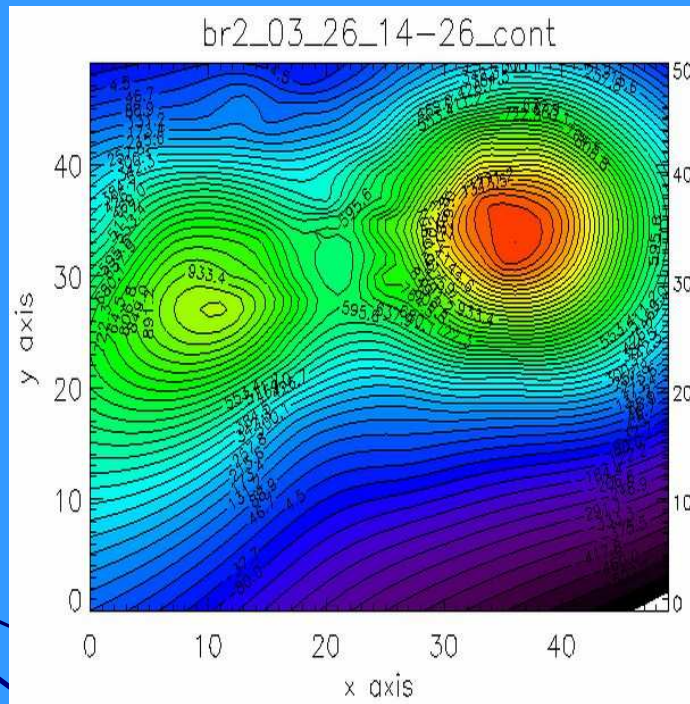
Senior Scientific



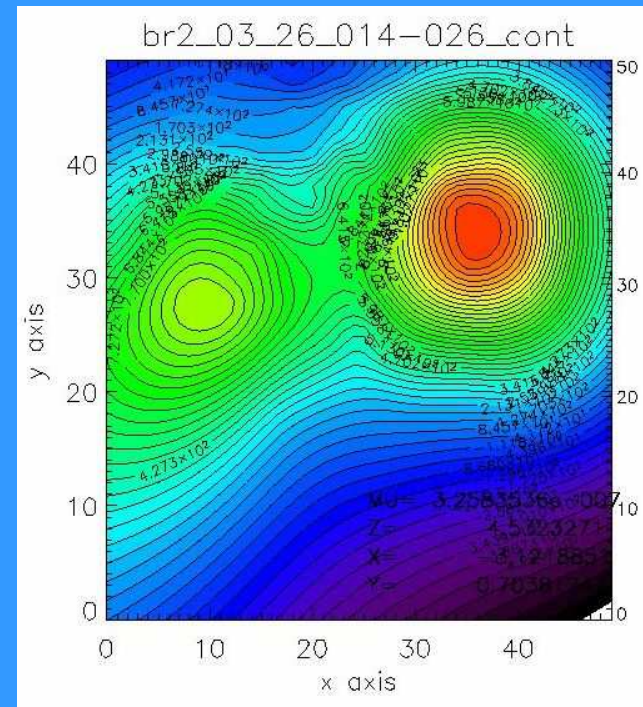
The University of New Mexico

Localization of Nanoparticle Sources in the Brain

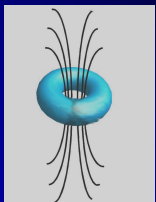
Experimental Fields



Theoretical Fields



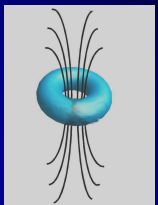
Dipole1:	X	Y	Z	M	N
	-3.12	0.70	4.53	3.26	
			7.2E+10		
Dipole2:	X	Y	Z	M	
	2.19	1.85	4.31	4.07	



Senior Scientific

Alzheimer Disease Status

- 1) Primary Imaging analysis completed
- 2) Antibodies for Amyloid Plaque and Tau
- 3) Antibodies coupled to Nanoparticles
- 4) Flash-frozen brain slices of AD Patients
- 5) AD Mouse model under development
(UMN have developed AD mouse)



Summary

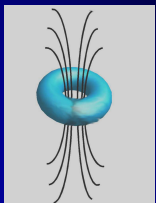
- (1) SQUID sensor sensitivity can detect and image brain magnetic fields and targeted nanoparticles in disease.
- (2) Measurement of natural biomagnetic fields can be used to understand brain function
- (3) Measurement of natural biomagnetic fields can be used to understand the working mind
- (4) Magnetic nanoparticles and weak field sensors can be used for early disease detection.
- (5) Nanoparticle applications include cancer, leukemia, transplant rejection, and brain diseases.
- (6) Treatment options include multi-function nanoparticles for localization and magnetic concentration or hyperthermia.

This research was funded in part by:

The National Cancer Institute

The National Institute for Allergies and
Infectious Disease

The US Department of Defense



Senior Scientific



The University of New Mexico

Primary Participants

E. R. Flynn¹,

H. C. Bryant^{1,3},

D. A. Sergatskov^{1,4},

R. S. Larson³, D. Lovato³, L. Sillerud³, J. Jaetao³

N. Adolphi²

C. Bergemann⁵

D. Huber⁶

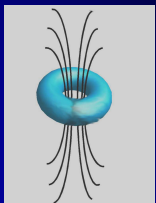
A. Georgopoulos⁷, A. Leuthold⁷

¹Senior Scientific, LLC, ²New Mexico Resonance

³University of New Mexico, ⁴FermiLab,

⁵Chemicell GmbH, Germany, ⁶CINT-Sandia National Lab,

⁷VVA Hospital and UMN, Minneapolis, MN



Senior Scientific



The University of New Mexico